ORIGINAL PAPER



A REE-in-plagioclase-clinopyroxene thermometer for crustal rocks

Chenguang Sun^{1,2,3} • Yan Liang¹

Received: 20 July 2016 / Accepted: 22 December 2016 © Springer-Verlag Berlin Heidelberg 2017

Abstract A REE-in-plagioclase-clinopyroxene thermometer has been developed on the basis of the temperatureand composition-dependent rare-earth element (REE) partitioning between coexisting plagioclase and clinopyroxene. This two-mineral exchange thermobarometer is constructed using parameters from lattice strain models for REE+Y partitioning in plagioclase and in clinopyroxene that were independently calibrated against experimentally determined mineral-melt partitioning data. An important advantage of this REE-based thermometer is that it can provide accurate temperatures through linear least-squares analysis of REE+Y as a group. Applications of the REE-in-plagioclase-clinopyroxene thermometer to volcanic and cumulate rocks show that temperatures derived from the new thermometer agree well with independently constrained magma crystallization temperatures, which adds confidence to applications of the REE-exchange thermometer to natural rocks with a wide spectrum of composition (i.e., from basalt to rhyolite). However, systematic temperature

Communicated by Timothy L. Grove.

Electronic supplementary material The online version of this article (doi:10.1007/s00410-016-1326-9) contains supplementary material, which is available to authorized users.

Chenguang Sun csun@rice.edu

Published online: 01 April 2017

- Department of Earth, Environmental and Planetary Sciences, Brown University, Box 1846, Providence, RI 02912, USA
- Department of Geology and Geophysics, Woods Hole Oceanographic Institution, Woods Hole, MA 02543, USA
- Present Address: Department of Earth Science, Rice University, 6100 Main Street, MS-126, Houston, TX 77005, USA

differences appear between the REE- and Mg-exchange thermometers for the volcanic and cumulate rocks. Through numerical simulations of diffusion in plagioclase-clinopyroxene systems, we demonstrate that (1) due to their slower diffusion rates, REE in minerals preferentially records crystallization or near-crystallization temperatures of the rock, and that (2) Mg is readily rest to lower temperatures for rocks from intermediately or slowly cooled magma bodies but records the initial crystallization temperatures of rocks from rapidly cooled magmas. Given their distinct diffusive responses to temperature changes, REE and Mg closure temperatures recorded by the two thermometers can be used in concert to study thermal and magmatic histories of plagioclase- and clinopyroxene-bearing rocks.

Keywords REE geothermometry · Plagioclase · Clinopyroxene · Crystallization temperature · Diffusive response · Geospeedometry

Introduction

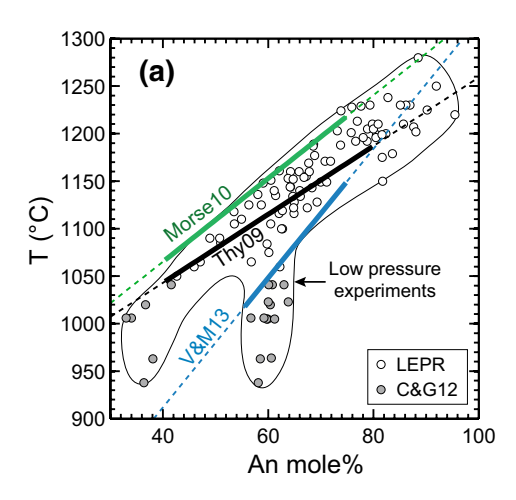
Plagioclase and pyroxene are common rock-forming minerals formed over a broad range of temperature and pressure in igneous rocks. Quantitative determination of equilibrium or crystallization temperatures for plagioclase- and pyroxene-bearing rocks is crucial to the interpretation of the thermal and magmatic histories of these rocks. Many attempts have been made to determine crystallization temperatures of plagioclase in silicate melts since the pioneering study of Kudo and Weill (1970). Following their approach, semi-empirical thermodynamic models have been calibrated as thermometers based on the plagioclase-melt equilibria (e.g., Mathez 1973; Glazner 1984; Putirka 2005, 2008; Lange et al. 2009; Waters and Lange 2015). According to

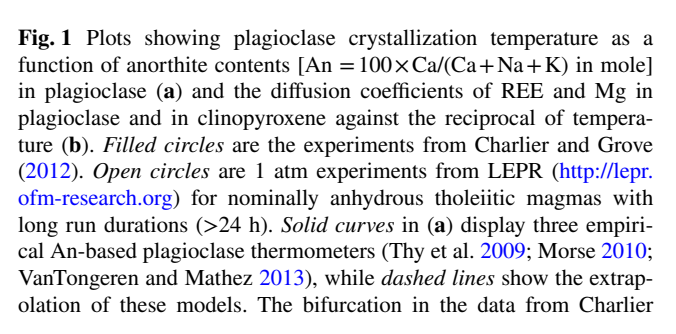


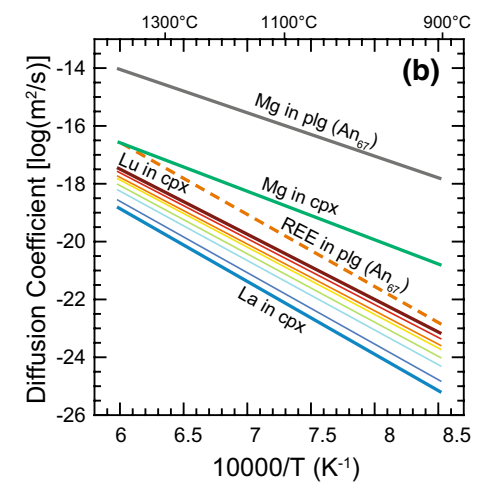
these models, plagioclase saturation in silicate melts is a function of temperature, pressure, and melt composition (including water abundance). Thus, applications of these thermometers are limited to phenocrysts with coexisting quenched melts or melt inclusions and also require independent constraints of water content in the equilibrium melt.

Empirical thermometers have also been developed for selected compositional ranges by calibrating the equilibrium temperature as a function of anorthite content [An $=100\times Ca/(Ca+Na+K)$, in mole] in plagioclase (e.g., Thy et al. 2009; Morse 2010; VanTongeren and Mathez 2013). These An-based thermometers are useful to estimate crystallization temperatures of mafic cumulate rocks, but may involve large uncertainties without proper constraints on cumulate parental magmas. Due to the effect of melt composition, temperatures of the low-pressure experiments can vary up to 200 °C for a given plagioclase composition (Fig. 1a). Thus, care should be taken when applying the An-based thermometers to cumulate rocks. Recently, Faak et al. (2013) developed a new thermometer based on Mg exchange between plagioclase and clinopyroxene. As shown in Faak et al. (2014), Mg distribution in plagioclase is sensitive to a wide range of cooling rates (e.g., >0.1-10⁻⁴ °C/year) because of its fast diffusion in plagioclase (Fig. 1b). Hence, the Mg-based thermometer is incapable of recording the initial crystallization temperatures unless the cooling rate is very fast.

It has been long recognized that the distribution of trace elements between two coexisting minerals depends on temperature, pressure, and mineral compositions (e.g., Stosch 1982; Seitz et al. 1999; Witt-Eickschen and O'Neill 2005; Lee et al. 2007; Liang et al. 2013; Sun and Liang 2014, 2015). Based on lattice strain models for rare-earth element (REE) partitioning in pyroxenes and garnet (Sun and Liang 2012, 2013a, b; Yao et al. 2012), we recently developed a REE-in-two-pyroxene thermometer (Liang et al. 2013) and a REE-in-garnet-clinopyroxene thermobarometer (Sun and Liang 2015). Applications of these REE-exchange thermometers to well-characterized field samples from the literature demonstrated that REE record higher temperatures than major divalent cations (i.e., Ca²⁺, Mg²⁺, and Fe²⁺) for mafic and ultramafic rocks from cooling environments (e.g., Liang et al. 2013; Dygert and Liang 2015; Sun and Liang 2015; Wang et al. 2015) but preferentially record lower temperatures for rocks from thermally perturbed environments (Sun and Liang 2015). Through simple diffusion modeling and closure temperature consideration for cooling bi-mineralic systems (Liang 2015; Yao and Liang 2015), the former is attributed to slower diffusion of REE in minerals (e.g., Cherniak 2010; Cherniak and Dimanov 2010; Fig. 1b). Given the short time-scales of low-pressure







and Grove (2012) is due to liquid immiscibility. The diffusion coefficients of La, Ce, Nd, Dy, and Yb in clinopyroxene were calculated for 2 kbar using the diffusion parameters from Van Orman et al. (2001), while those of other REE were interpolated according to their ionic radii. Because REE diffusion coefficients in plagioclase do not appear to vary with ionic radii, the Nd diffusion parameters from Cherniak (2003; An = 67) were used to describe REE diffusion coefficients in plagioclase. Mg diffusion parameters for plagioclase are from Van Orman et al. (2014), and those for clinopyroxene are from Müller et al. (2013)



magma solidification (e.g., <200 kyr solidification time for the Bushveld Complex; Cawthorn and Webb 2013) and hence relatively rapid cooling, REE-based thermometers can potentially record crystallization or near-crystallization temperatures of rocks from shallow magma bodies.

In this study, we present a new thermometer based on REE exchange between plagioclase and clinopyroxene. The exchange reaction is quantified by a new lattice strain model, in which the parameters were independently calibrated against experimentally determined clinopyroxenemelt and plagioclase-melt partitioning data (Sun and Liang 2012; Sun et al. 2017). Using compositions of coexisting plagioclase and clinopyroxene in volcanic and cumulate rocks reported in the literature, we show that this new REE-based thermometer records plagioclase crystallization temperatures during magma solidification and is resistant to diffusive resetting. Furthermore, through diffusion modeling, we demonstrate that combining this REE-based thermometer with the Mg-exchange thermometer (Faak et al. 2013) can place constraints on the cooling rate and residence time of crustal magma bodies.

Developing a REE-in-plagioclase-clinopyroxene thermometer

Theoretical basis

The theoretical basis of exchange thermometers or barometers is the temperature- and pressure-dependent exchange reaction of an element of interest between coexisting minerals, which takes the simple thermodynamic expression:

$$ln D = A + \frac{B - f(P)}{T},$$
(1)

where D is the partition coefficient of the element defined by the concentration ratio of the element in the two minerals; A and B are coefficients corresponding to the changes of entropy and enthalpy; and f(P) is a pressure correction term for the exchange reaction. Equation (1) has also been used to describe the partitioning of trace elements between a pair of coexisting minerals (e.g., Stosch 1982; Seitz et al. 1999; Witt-Eickschen and O'Neill 2005; Lee et al. 2007; Liang et al. 2013; Sun and Liang 2014, 2015). For a temperature or pressure sensitive exchange reaction, Eq. (1) can be effectively used as a thermometer or barometer, when the coefficients A and B and f(P) are calibrated experimentally. Rearranged to a linear form for a group of geochemically similar elements, such as REE, Eq. (1) allows constraints of temperature and pressure by fitting the partitioning data of multiple elements to the expression:

$$B_j = T(\ln D_j - A_j) + f(P), \tag{2}$$

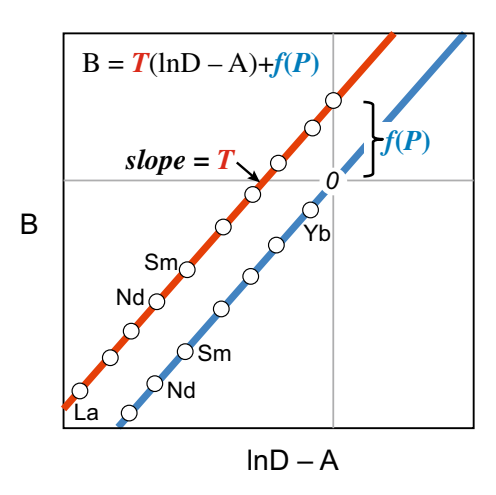


Fig. 2 Schematic diagram showing the basic idea of REE-in-two-mineral thermometers or thermobarometers

where j is an element in the group. As illustrated in Fig. 2, in a plot of $(\ln D - A)$ vs. B, all elements in the group theoretically should define a straight line intercepting Y-axis at f(P). When the effects of temperature and pressure are both significant, the equilibrium temperature and pressure can be obtained from the slope and intercept of this line (red line in Fig. 2). This is the case for the REE-in-garnetclinopyroxene thermobarometer (Sun and Liang 2015). When pressure effect is negligible or relatively small, f(P)may vanish or become unimportant, so that accurate determination of pressure is not possible. For a relatively small pressure effect, f(P) may be integrated into the coefficient B. Accordingly, the straight line should pass through the origin (blue line in Fig. 2), and thus, only temperature can be obtained from the slope. This is the case for the REE-intwo-pyroxene thermometer (Liang et al. 2013). To develop a REE-in-plagioclase-clinopyroxene thermometer, one has to quantitatively determine the temperature, pressure, and composition effects on REE partitioning between the two minerals.

Plagioclase-clinopyroxene REE partitioning model

The exchange of REE and Y between plagioclase and clinopyroxene can be described by the partition coefficient that follows the lattice strain model for two coexisting minerals (Lee et al. 2007; Liang et al. 2013; Sun and Liang 2014):

$$D_{j}^{\text{plg-cpx}} = \frac{D_{0}^{\text{plg}}}{D_{0}^{\text{cpx}}} \exp \left[-\frac{4\pi N_{A} E^{\text{plg}}}{RT} \left(\frac{r_{0}^{\text{plg}}}{2} \left(r_{0}^{\text{plg}} - r_{j} \right)^{2} - \frac{1}{3} \left(r_{0}^{\text{plg}} - r_{j} \right)^{3} \right) + \frac{4\pi N_{A} E^{\text{cpx}}}{RT} \left(\frac{r_{0}^{\text{cpx}}}{2} \left(r_{0}^{\text{cpx}} - r_{j} \right)^{2} - \frac{1}{3} \left(r_{0}^{\text{cpx}} - r_{j} \right)^{3} \right) \right]$$
(3)



where $D_j^{\mathrm{plg-cpx}}$ is the partition coefficient of element j between plagioclase (plg) and clinopyroxene (cpx); D_0 is the partition coefficient for strain-free substitution; r_0 is the ionic radius of the strain-free cation, r_j is the ionic radius of element j; E is the apparent Young's modulus for the lattice site; N_A is Avogadro's number; T is temperature in K; and R is the gas constant. The lattice strain parameters (D_0 , r_0 and E) are the same as those in the lattice strain model for mineral-melt systems (Blundy and Wood 1994), and can be parameterized as a function of temperature, pressure, and composition using experimentally determined mineral-melt REE + Y partitioning data.

Recently, Sun and Liang (2012) and Sun et al. (2017) developed new lattice strain models for REE partitioning between clinopyroxene and basaltic melt and between plagioclase and basaltic to dacitic melts, respectively. To ensure the quality of the partitioning data and hence the accuracy of the model, they calibrated the lattice strain parameters against carefully selected partitioning experiments for clinopyroxene (43 experiments) and plagioclase (29 experiments). These selected experiments cover a wide range of temperature, pressure, and compositions (supplementary Tables S1–S2). Specifically, the 43 clinopyroxenemelt partitioning experiments cover temperatures from 1042 to 1470 °C, pressures from 1 atm to 4 GPa, and clinopyroxene Mg# $[=100 \times Mg/(Mg + Fe)$ in mole] from 54 to 100 (Fig. 3a). The 29 plagioclase-melt partitioning experiments were conducted at temperatures of 1127 to 1410 °C and pressures of 1 atm to 1.5 GPa and produced plagioclase with An from 41 to 98 (Fig. 3b). Both experimental data sets cover a wide range of hydrous conditions.

For REE+Y partitioning between clinopyroxene and melt, the lattice strain parameters take the following expressions (Sun and Liang 2012):

$$\begin{split} \ln D_0^{\rm cpx} &= -7.14(\pm 0.53) + \frac{7.19(\pm 0.73) \times 10^4}{RT} \\ &+ 4.37(\pm 0.47) X_{\rm Al}^{\rm T,cpx} + 1.98(\pm 0.36) X_{\rm Mg}^{\rm M2,cpx} \\ &- 0.91(\pm 0.19) X_{\rm H_2O}^{\rm melt}, \end{split} \tag{4a}$$

$$\begin{split} r_0^{\rm cpx}\left(\mathring{\rm A}\right) &= 1.066(\pm 0.007) - 0.104(\pm 0.035) X_{\rm Al}^{\rm M1,cpx} \\ &- 0.212(\pm 0.033) X_{\rm Mg}^{\rm M2,cpx} \end{split} \tag{4b}$$

$$\begin{split} E^{\rm cpx}({\rm GPa}) &= \left[2.27(\pm 0.44)r_0^{\rm cpx} - 2.00(\pm 0.44)\right] \times 10^3, \quad (4\text{c}) \\ \text{where } X_{\rm Al}^{\rm T,cpx} \text{ is the Al content in the tetrahedral site per formula unit; } X_{\rm Al}^{\rm M1,cpx} \text{ is the Al content in the M1 site; } X_{\rm Mg}^{\rm M2,cpx} \\ \text{is the Mg content in the M2 site calculated assuming a random Fe-Mg distribution over the M1 and M2 sites; } X_{\rm H_2O}^{\rm melt} \text{ is the molar fraction of H}_2{\rm O} \text{ in the melt calculated using the} \end{split}$$

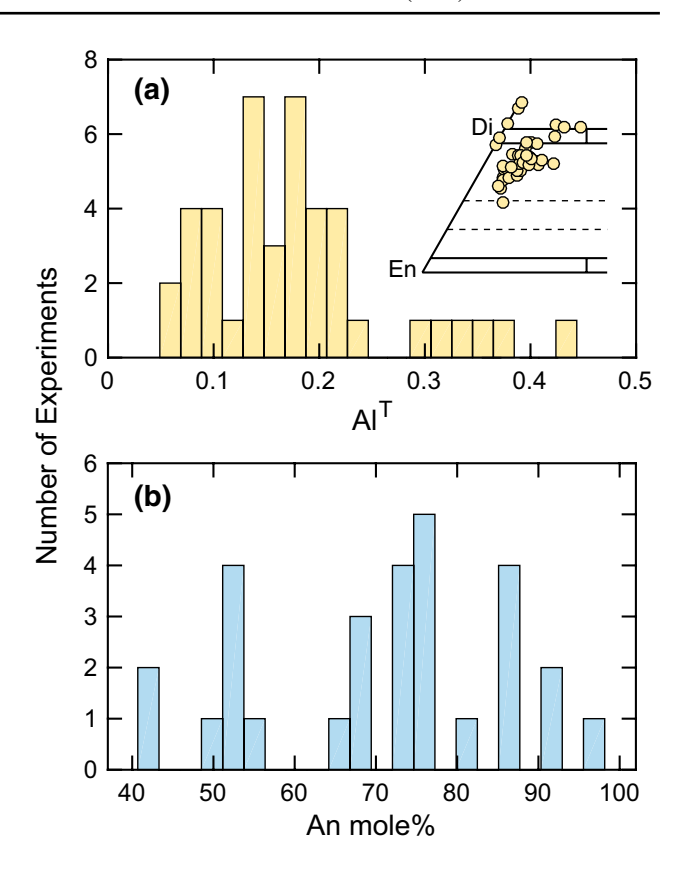


Fig. 3 Histograms showing the compositional variations of clinopyroxene and plagioclase from the mineral-melt partitioning experiments used in model calibrations: (a) tetrahedrally coordinated Al (Al^T) in clinopyroxene (per six-oxygen) and (b) anorthite content in plagioclase. Inset in (a) is part of the pyroxene quadrilateral showing clinopyroxene compositions. Di and En denote diopside and enstatite end-members, respectively. Sources of the experimental data are provided in Sun and Liang (2012) and Sun et al. (2017) and are also summarized in supplementary Tables S1 and S2

approach of Wood and Blundy (2002); and numbers in parentheses are 2σ uncertainties derived from the calibration. All iron is assumed as Fe²⁺ for pyroxene formula calculations. Equation (4a–c) indicate that temperature and pyroxene composition (i.e., Al and Mg) primarily determine REE+Y partitioning between clinopyroxene and melt. The effect of water becomes important under hydrous conditions. Although pressure and melt composition (other than water) do not appear in Eq. (4a–c), they may also influence REE partitioning through pyroxene-melt phase equilibria.

For REE+Y partitioning between plagioclase and melt, the lattice strain parameters can be described as (Sun et al. 2017) follows:

$$\ln D_0^{\text{plg}} = 16.05(\pm 1.57) - \frac{19.45(\pm 1.78) + 1.17(\pm 0.14)P^2}{RT} \times 10^4 - 5.17(\pm 0.37) \left(X_{\text{Ca}}^{\text{plg}}\right)^2,$$
 (5a)



$$r_0^{\text{plg}} (\text{Å}) = 1.179(\pm 0.027),$$
 (5b)

$$E^{\text{plg}}(\text{GPa}) = 196(\pm 51),$$
 (5c)

where $X_{\rm Ca}^{\rm plg}$ is the Ca content in plagioclase per eight-oxygen; and P is pressure in GPa. Equation (5a–c) indicate that temperature, pressure, and Ca content in plagioclase (similar to An) dominate REE+Y partitioning in plagioclase. As plagioclase composition and saturation temperature depend on melt composition and water content (e.g., Putirka 2005; Lange et al. 2009; Namur et al. 2012; Almeev et al. 2012; Waters and Lange 2015), the effect of major element composition and water in the melt on REE partitioning may exert through plagioclase-melt phase equilibria.

Combining with the lattice strain parameters for REE+Y partitioning in clinopyroxene (Eq. 4a-c) and in plagioclase (Eq. 5a-c), Eq. (3) can be used to quantitatively determine the effects of temperature, pressure, and composition on REE+Y distribution between coexisting plagioclase and clinopyroxene. Note that $X_{H_2O}^{\text{melt}}$ from Eq. (4a) is the only melt composition term in the model but can be neglected under subsolidus or anhydrous magmatic conditions. According to the clinopyroxene-melt partitioning experiments compiled in Sun and Liang (2012), 10 wt% water in the melt is equivalent to 0.6 molar fraction of water $(X_{H_2O}^{\text{melt}})$. To examine the relative significance of temperature and compositional factors, we calculated REE+Y partition coefficients for a wide range of temperature (850-1250 °C), pressure (1 atm to 1 GPa), composition $(X_{\text{Ca}}^{\text{plg}} = 0.4 - 0.8, X_{\text{Al}}^{\text{T,cpx}} = 0.04 - 0.4,$ and 0-10 wt% H₂O in the melt). The mineral compositions from Norman et al. (2005; KIL55-2) are taken as a reference.

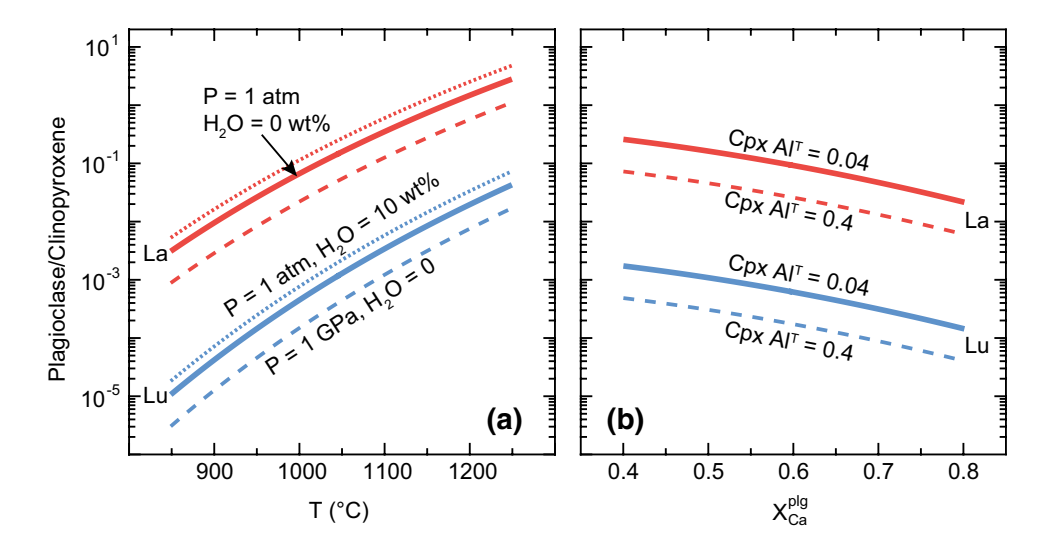
Figure 4 displays the calculated plagioclase-clinopyroxene partition coefficients for La (red curves) and Lu (blue curves) that bracket the variations of partition coefficients for all REE+Y. For the given set of mineral major element compositions, a 400 °C increase in temperature (from 850 °C to 1250 °C) raises plagioclase-clinopyroxene REE+Y partition coefficients by three to four orders of magnitude, while an increase of pressure from 1 atm (solid curves) to 1 GPa (dashed curves in Fig. 4a) reduces the REE+Y partition coefficients by a factor of three. Assuming that the plagioclase and clinopyroxene coexist with silicate magmas, addition of 10 wt% water in the melt (dotted curves in Fig. 4a) increases the partition coefficients by less than a factor of two. For a given temperature (1000 °C) and pressure (1 atm), an increase of Ca content (X_{Ca}^{plg}) in plagioclase from 0.4 to 0.8 lowers the partition coefficients by one order of magnitude (solid curves in Fig. 4b), equivalent to a ~100 °C decrease in temperature, while an increase of $X_{Al}^{T,cpx}$ from 0.04 to 0.4 reduces the partition coefficients by about a factor of four (dashed curves in Fig. 4b). Overall, the effects of pressure and water are small, those of mineral compositions are small to moderate, and the temperature effect appears to be the most significant. The considerable temperature effect is consistent with its large coefficient in Eq. (5a) and allows us to develop a new thermometer based on REE+Y partitioning between plagioclase and clinopyroxene.

A REE-in-plagioclase-clinopyroxene thermometer

Rearranging Eq. (3) to the form of Eq. (2), we obtain a new thermometer based on REE+Y distribution between plagioclase and clinopyroxene that takes the following expressions:

$$B_j = T(\ln D_j - A), \tag{6a}$$

Fig. 4 Variations of La and Lu partition coefficients between plagioclase and clinopyroxene as a function of temperature (a) and Ca content in plagioclase (b). Partition coefficients were calculated using Eqs. (3) and (6a-c)





$$A = 23.19 - 5.17 \left(X_{\text{Ca}}^{\text{plg}}\right)^{2} - 4.37X_{\text{Al}}^{\text{T,cpx}} - 1.98X_{\text{Mg}}^{\text{M2,cpx}} + 0.91X_{\text{H}_{2}\text{O}}^{\text{melt}},$$
(6b)

$$B_j = -32.04 \times 10^3 - 1.41 \times 10^3 P^2 + 909.85 G(r_j),$$
 (6c)

$$G(r_{j}) = -E^{\text{plg}} \left(\frac{r_{0}^{\text{plg}}}{2} \left(r_{0}^{\text{plg}} - r_{j} \right)^{2} - \frac{1}{3} \left(r_{0}^{\text{plg}} - r_{j} \right)^{3} \right) + E^{\text{cpx}} \left(\frac{r_{0}^{\text{cpx}}}{2} \left(r_{0}^{\text{cpx}} - r_{j} \right)^{2} - \frac{1}{3} \left(r_{0}^{\text{cpx}} - r_{j} \right)^{3} \right).$$
 (6d)

The coefficient A depends strongly on major element compositions of plagioclase and clinopyroxene, while the coefficient B is a function of clinopyroxene major element composition, ionic radii of REE, and pressure. Note that G is a correction term for the lattice strain changes of individual elements. Since the pressure effect is relatively small, no attempt is made to retrieve pressure here, and the pressure term is lumped into the coefficient B in Eq. (6c). The $X_{\rm H_2O}^{\rm melt}$ term in Eq. (6b) can be neglected, except when plagioclase and clinopyroxene coexist with hydrous magmas (e.g., volcanic phenocrysts with hydrous melt inclusions).

Given the major element and REE compositions of coexisting plagioclase and clinopyroxene, one can calculate temperature through the steps similar to those for other REE-based two-mineral thermometers (Liang et al. 2013; Sun and Liang 2015): (1) calculate coefficients A and B using Eq. (6b-d), mineral major element compositions, and a relevant pressure; (2) examine REE+Y abundances in plagioclase and clinopyroxene in a spider diagram to exclude obvious outliers; (3) perform linear least-squares regression analysis of plagioclase-clinopyroxene REE+Y partition coefficients in the plot of $(\ln D - A)$ vs. B to determine the slope of the straight line passing through the origin, i.e., the temperature. The uncertainties of the estimated temperature can be obtained through the linear least-squares analysis. The multiple-element approach of the REE-based thermometer also allows exclusion of outliers, reducing uncertainties of estimated temperatures through a robust linear least-squares regression method. In the online Supplementary Materials, an Excel program is provided for interested readers to calculate temperature using the REE-in-plagioclase-clinopyroxene thermometer.

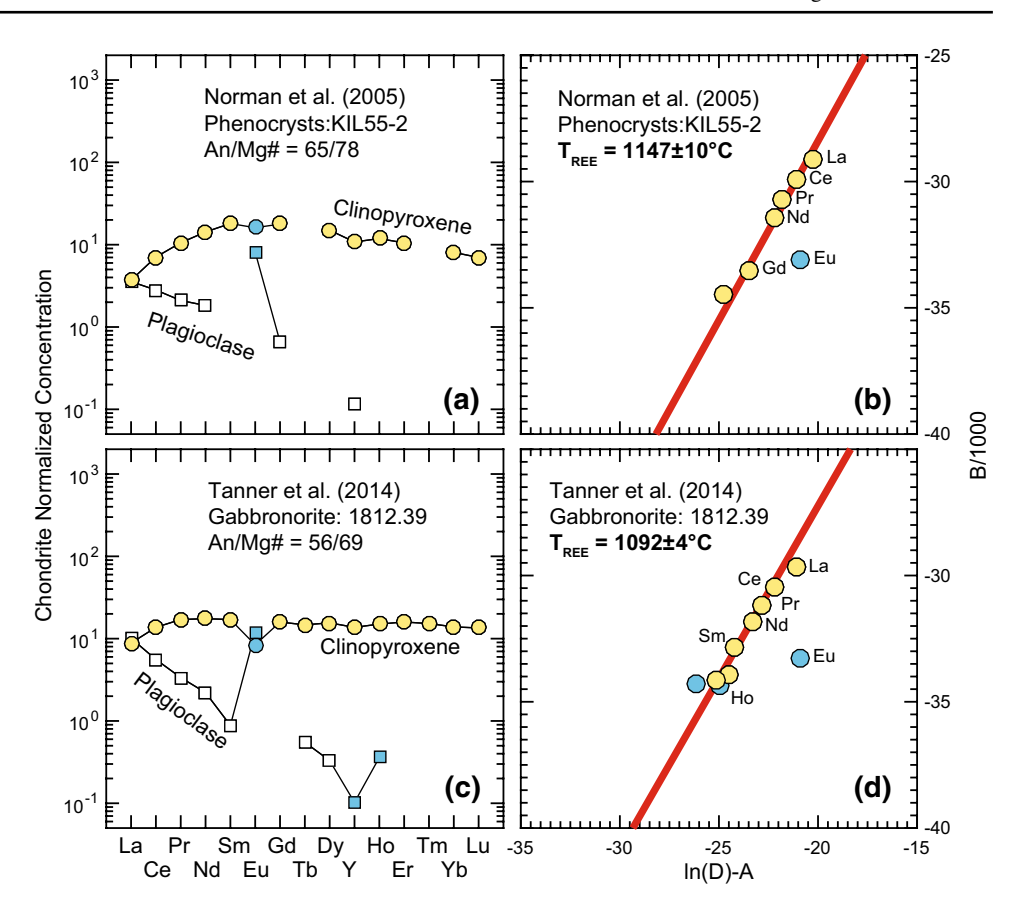
To demonstrate the temperature calculation, here, we applied this new REE-based thermometer to coexisting plagioclase and clinopyroxene in a volcanic rock (KIL 55-2) from the 1955 eruption of the Kilauea volcano, Hawaii (Norman et al. 2005) and in a gabbro (1812.39) from the Upper Main Zone (UMZ) in the Northern Limb of the Bushveld Complex (Tanner et al. 2014). According

to Norman et al. (2005), plagioclase and clinopyroxene in this volcanic lava are phenocrysts in chemical equilibrium with the finely quenched mesostasis at temperatures about 1127-1147 °C and pressures < 3 kbar. The water abundance in the volcanic lava was not reported in Norman et al. (2005) but is likely < 0.5 wt% as indicated by olivine-hosted melt inclusions from earlier and later eruptions at the Kilauea volcano (Anderson and Brown 1993; Barsanti et al. 2009). Based on the volatile contents in the olivine-hosted melt inclusions, Barsanti et al. (2009) calculated the crystallization pressures at 0.02–0.62 kbar with an average of 0.20 ± 0.16 kbar, which are comparable to those estimated by Anderson and Brown (1993). However, crystallization temperatures, pressures, and water contents of the Bushveld UMZ parental magmas have not been determined previously. Assuming that the volcanic lava and the gabbro were crystalized at 0.2 kbar with 0.5 wt% H₂O in the melt and 2 kbar under an anhydrous condition, respectively, we perform temperature inversions following the aforementioned steps as illustrated in Fig. 5.

Both samples display enriched REE patterns in clinopyroxene but depleted REE patterns in plagioclase (Fig. 5a, c). Because heavy REE are strongly incompatible in plagioclase, their abundances in plagioclase are close to or below detection limits. The abnormally low Y abundance in plagioclase of the gabbro is likely due to the large analytical error. As Eu is mainly present as a divalent cation in plagioclase, it is systematically apart from other REE in the spider diagram. In the temperature inversion diagrams (Fig. 5b, d), Eu is still peculiar in both samples as well as Y + Ho in the volcanic rock, and therefore, they are excluded from the temperature calculations. Using a robust linear least-squares regression method, we draw a straight line passing through the remaining REE and the origin and obtain the temperature from the slope for each sample. Interestingly, for the volcanic rock, the inverted temperature $(1147 \pm 10 \,^{\circ}\text{C})$ is equivalent to that $(1140 \pm 20 \,^{\circ}\text{C})$ derived from the Mgexchange thermometer of Faak et al. (2013), and both are comparable with the crystallization temperature (1127–1147 °C) suggested by Norman et al. (2005). This indicates that the REE-based thermometer likely records magmatic temperatures. For the gabbro sample, the temperature (1092 ± 4 °C) determined by the REE-based thermometer is $281 \,^{\circ}\text{C}$ greater than that $(814 \pm 20 \,^{\circ}\text{C})$ calculated using the Mg-based thermometer. The significant temperature difference for this gabbro may be due to diffusive resetting of Mg between coexisting plagioclase and clinopyroxene.



Fig. 5 Examples of temperature inversions for volcanic phenocrysts (KIL55-2) from the Kilauea Volcano, Hawaii (Norman et al. 2005) and a gabbro (1812.39) from the Bushveld Complex (Tanner et al. 2014). Plots (a) and (c) are spider diagrams showing the chondritenormalized REE abundances in clinopyroxene and plagioclase, and (b) and (d) are temperature inversion diagrams showing the linear least-squares regression analyses of the REE partitioning data. The thick red lines are the best-fit lines passing through the origin (cf. Eq. 6a). Chondrite values are taken from Anders and Grevesse (1989). Errors of the inverted temperatures are derived from the regression analyses without considering the REE analytical uncertainties. Cyan markers indicate outliers excluded from the temperature inversions



Sources of uncertainties in the calculated temperatures

The accuracy of the REE-in-plagioclase-clinopyroxene thermometer depends on uncertainties of chemical analyses, knowledge of crystallization pressures and hydrous conditions, and validity of co-crystallization of plagioclase and clinopyroxene. Here, we assess the sources of uncertainties and show that different crystallization sequences of plagioclase and clinopyroxene may introduce significant errors in the calculated temperatures.

Chemical analyses

It is widely accepted that major element abundances of minerals can be accurately determined through electron microprobe analyses; however, large uncertainties remain on REE analyses for mafic minerals (e.g., plagioclase, orthopyroxene, and olivine). Particularly, middle and heavy REE are strongly incompatible in plagioclase and often below detection limits (cf. Fig. 5). To assess the effect of analytical errors on the calculated temperatures, here, we carried out Monte Carlo simulations using the major and trace element compositions of two samples from Namur et al. (2011) (DC-9-468: An =48; DC-9-2410: An =68) as the initial inputs. Because heavy REE in plagioclase

from these two samples were below their detection limits, we calculated all REE abundances in plagioclase based on those in clinopyroxene using temperatures derived from the REE-based thermometer and the plagioclase-clinopyroxene partitioning model (Eq. 3). Random errors with a normal distribution were assigned to REE abundances in plagioclase to simulate analytical uncertainties. For each sample, we generated 1000 sets of plagioclase-clinopyroxene pairs with a given percentage error between 0 and 50% and then calculated temperature for each pair using this REE-based thermometer. A representative example of temperature inversion for 50% random errors is shown in supplementary Fig. S1. As middle and heavy REE are highly depleted in plagioclase from natural rocks, we also calculated temperatures by excluding heavy REE in plagioclase or excluding middle and heavy REE in plagioclase. The standard deviations of the calculated temperatures manifest the temperature uncertainties derived from different analytical errors. When all REE in plagioclase are above the detection limits, uncertainties in the calculated temperatures are within ±15°C for <50% analytic errors of REE in plagioclase (black curves in Fig. 6a). When heavy REE are excluded, the temperature uncertainties marginally increase by up to 5°C for 50% analytic errors (blue curves in Fig. 6a). However, temperatures calculated using only light REE have larger uncertainties up to about ± 30 °C



for 50% analytic errors (red curves in Fig. 6a). Assuming 30% analytic errors for REE in plagioclase, the new REE-based thermometer can accurately determine temperatures to within $\pm\,10\,^{\circ}\text{C}$.

Crystallization pressure and hydrous conditions

Crystallization pressure and melt water contents are required to estimate temperatures using this new REEbased thermometer, but they are difficult to constrain independently for field samples. As demonstrated in the temperature inversion examples in section "A REE-in-plagioclase-clinopyroxene thermometer", relevant pressures and melt water contents may be assumed for temperature calculations, which likely introduces additional uncertainties. To assess the influences of pressure and water on the temperatures, we calculated temperatures for the aforementioned two samples (DC-9-468 and DC-9-2410 from Namur et al. 2011) by assuming a range of pressures (0–10 kbar) and melt water abundances (0-10 wt%). With reference to 0 kbar and 0 wt% water (T₀ in Fig. 6b), the calculated temperature increases by ~60°C for a pressure increase from 0 to 10 kbar but decreases by ~30°C for addition of water from 0 to 10 wt% in the melt (Fig. 6b). The overall variations of the calculated temperature are about ± 10 °C for a pressure uncertainty of ±4 kbar or for ±2 wt% errors of the estimated water content, indicating that the accuracy of this REE-based thermometer is insensitive to uncertainties of pressure and melt water content.

Crystallization sequences

The fundamental assumption for applying the new REEexchange thermometer to an igneous rock is that plagioclase and clinopyroxene were co-crystalized from the same parental magma. This is likely the case for a pair of cumulus crystals, a pair of intercumulus crystals, rims of the mineral pairs, and possibly cores of the mineral pairs at the thin-section scale. The corresponding temperatures of these pairs in a single cumulate rock can be significantly different because of their distinct crystallization histories. However, this co-crystallization assumption may become invalid in other cases, such as cumulus-intercumulus pairs and core-rim pairs. To estimate the effect of crystallization sequences, we calculated temperatures using plagioclase and clinopyroxene from different solidification stages during fractional crystallization of a mid-ocean-ridge basalt (MORB). MORB solidification was simulated using the MELTS program (Ghiorso and Sack 1995) for isobaric fractional crystallization of a primary MORB from Workman and Hart (2005) at 0.5 kbar under anhydrous condition. REE fractionation was calculated incrementally using the MELTS outputs and the partitioning models for olivine,

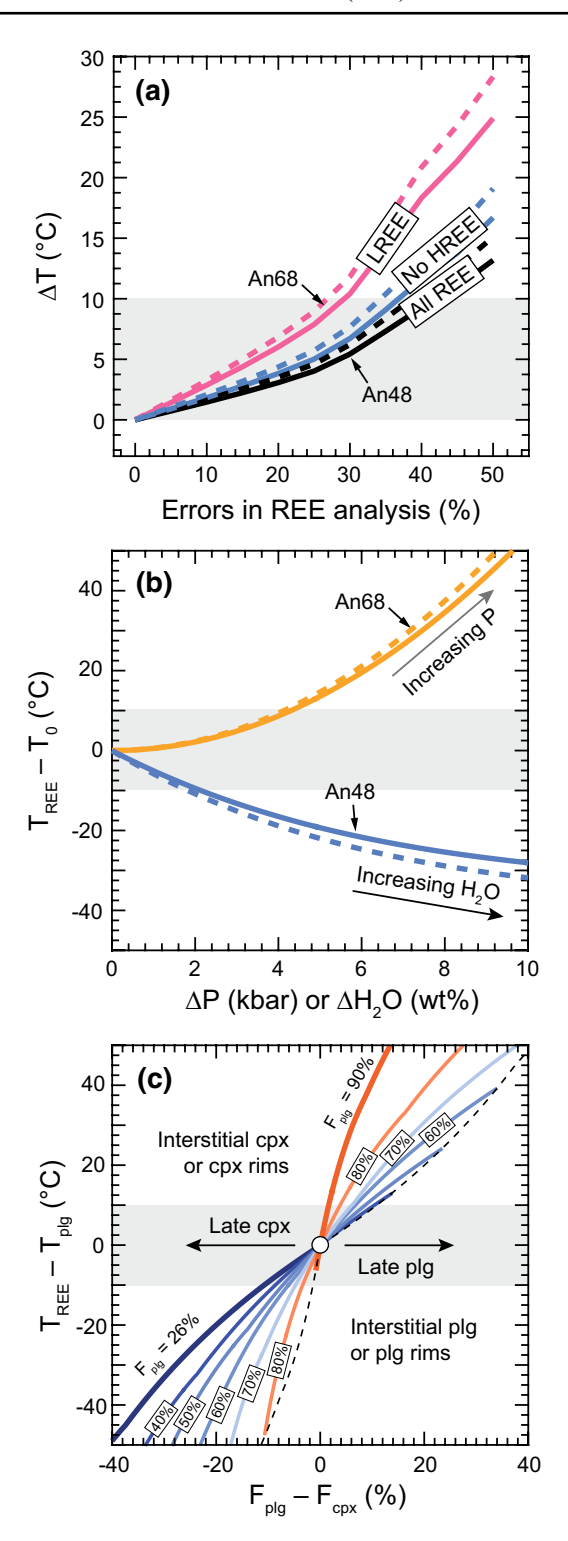


Fig. 6 Variations of uncertainties in the calculated temperatures (T_{REE}) as a function of REE analytical errors (**a**), pressure and water content (**b**), and relative crystallization sequences between plagioclase (F_{plg}) , degree of crystallization) and clinopyroxene (F_{cpx}) (**c**). Grey regions mark the $\pm 10\,^{\circ}\text{C}$ uncertainties of the calculated temperatures. In (**a**) and (**b**), *solid* and *dashed curves* indicate cases for plagioclase An₄₈ and An₆₈, respectively. *Solid curves* in (**c**) denote constant F_{plg} , whereas *dashed curves* enclose the lower boundary of the variations. See text for discussion



24

clinopyroxene, orthopyroxene, and plagioclase (Sun and Liang 2012, 2013a, 2014; Sun et al. 2017; Yao et al. 2012). Spinel is considered unimportant for fractionating REE. To mimic cumulus-intercumulus pairs and core-rim pairs, plagioclase was randomly coupled with clinopyroxene from different crystallization stages between 26% (i.e., the initial co-saturation) to 90% solidification of MORB. Applying the REE-based thermometer to randomly coupled plagioclase and clinopyroxene, we obtained the deviations of REE-derived temperatures from the plagioclase crystallization temperatures, which display a positive correlation with the relative crystallization sequences (Fig. 6c). Two representative examples of temperature inversion for randomly paired plagioclase and clinopyroxene are shown in supplementary Fig. S2.

The calculated temperatures for randomly paired plagioclase and clinopyroxene are determined by the apparent REE partition coefficients (\bar{D}) and the mineral major element compositions (cf. Eq. 6a-c). From 26 to 90% solidification of MORB, clinopyroxene compositional factors in A vary within a small range $(X_{\rm Al}^{\rm T}=0.08-0.10,~X_{\rm Mg}^{\rm M2}=0.08-0.17),$ whereas in plagioclase, it decreases from 0.77 to 0.40. As fractional crystallization proceeds from 26 to 90 %, REE abundances in plagioclase and in clinopyroxene increase by about factors of 5 to 10. The apparent negative correlation between Ca and REE abundances in plagioclase effectively reduces the variation of $ln(\bar{D})$ -A (cf. Eq. 6b-c) introduced by plagioclase, so that the calculated temperatures are not significantly influenced by the randomly picked plagioclase. Instead, when randomly picked clinopyroxene is paired with a given plagioclase, compositional factors could not compensate the variations of REE abundances in clinopyroxene. Hence, coupling plagioclase with an early (or late) clinopyroxene induces an overestimation (or underestimation) of the plagioclase crystallization temperature (Fig. 6c). The absolute deviation depends on the plagioclase composition in addition to the relative crystallization sequences between plagioclase and clinopyroxene. A more evolved plagioclase appears to induce a larger deviation of the REE-derived temperature from the plagioclase crystallization temperature. For plagioclase and clinopyroxene from the early stage fractional crystallization, a < 10 % relative crystallization sequence is required to ensure $a \pm 10$ °C uncertainty in the calculated temperature; however, for those from highly evolved magmas, more accurate estimation of the crystallization sequence is essential for a similar temperature uncertainty.

Although the initial crystallization sequences were set up by MORB fractional crystallization in a close system, the random coupling of minerals from different solidification stages also simulates possible dis-equilibrium mineral pairs in open systems, e.g., replenishments of primitive or evolved magmas derived from a similar initial melt. When the replenished magmas have distinct parental melts, errors in the REE temperatures for cumulus-intercumulus or core-rim pairs may become significant, and therefore, the REE temperatures may not provide any meaningful implications. Finally, it is worth noting that the preceding analysis is based on the MELTS program, which also has its own uncertainties in producing mineral crystallization sequences and compositions.

Field validation and applications

Volcanic and cumulate rocks are widespread in Earth's crust and often contain coexisting plagioclase and clinopyroxene. The crystallization temperatures of pre-eruptive volcanic lavas can be obtained from the widely used plagioclase-melt thermometers (e.g., Putirka 2005, 2008; Lange et al. 2009), whereas those of cumulate rocks have been estimated using the relationship between temperature and anorthite content in plagioclase for a selected compositional range (e.g., Thy et al. 2009; VanTongeren and Mathez 2013). When the major and trace element compositions of coexisting plagioclase and clinopyroxene were provided in addition to the major element compositions of equilibrium or parental melts, volcanic and cumulate rocks allow us to examine if temperatures derived from the REE-based thermometer are comparable to magma crystallization temperatures determined by the aforementioned independent approaches. Although the Mg-exchange thermometer is readily reset by diffusive re-equilibration (Faak et al. 2014), it provides lower limits of possible crystallization temperatures. In the following section, we use published field data to test if the REE-in-plagioclase-clinopyroxene thermometer can provide magma crystallization temperatures.

Volcanic rocks

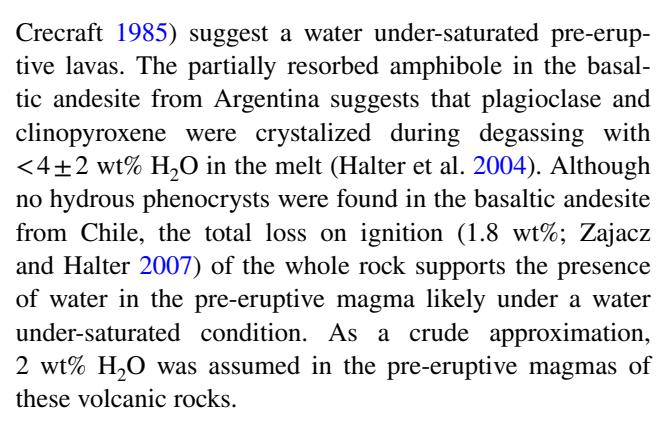
We compiled chemical data from 12 volcanic rocks with coexisting plagioclase and clinopyroxene phenocrysts from the Colima Volcanic Complex, Mexico (Luhr and Carmichael 1980), the Twin Peaks, Utah (Nash and Crecraft 1985), the Kilauea Volcano, Hawaii (Norman et al. 2005), the Farallón Negro Volcanic Complex, Argentina (Halter et al. 2004), the Villarrica Volcano, Chile (Zajacz and Halter 2007), White Island, New Zealand (Severs et al. 2009), and Campi Flegrei, Southern Italy (Fedele et al. 2009, 2015). The chemical compositions of quenched glass matrices and/or melt inclusions hosted in phenocrysts display



a wide spectrum (e.g., $SiO_2 = 51-72$ wt%; Mg# = 19-59), ranging from basalt, basaltic andesite, dacite, and rhyolite to phonolitic trachyte. The anorthite content in plagioclase phenocrysts ranges from 28 to 82 mol%, while Mg# and $X_{\Delta 1}^{\rm T}$ in clinopyroxene phenocrysts varies from 59 to 83 and from 0.01 to 0.11, respectively. In the two earlier studies (Luhr and Carmichael 1980; Nash and Crecraft 1985), trace element compositions of bulk phenocrysts were determined using instrumental neutron activation analyses of mineral separates. These minerals were carefully picked to avoid melt contamination (i.e., melt inclusions or adhering groundmass). In the more recent studies (Halter et al. 2004; Norman et al. 2005; Zajacz and Halter 2007; Severs et al. 2009; Fedele et al. 2009, 2015), average trace element compositions of phenocrysts were determined using laser ablation inductively coupled plasma mass spectrometry (LA-ICP-MS), which has better spatial resolution and lesser chance of melt contaminations. Zoning profiles of major and trace elements in phenocrysts were not reported in these studies.

Water contents in the pre-eruptive lavas are required in the plagioclase-melt thermometers, and can be estimated using melt inclusions from the same volcanoes, in which water abundances were determined by Fourier transform infrared spectroscopy (FTIR) or ion probes. Through wet chemical analyses, Luhr and Carmichael (1980) found 0.6 wt% H₂O retained in the most primitive andesite (Sample 15: $SiO_2 = 57.6$ wt%) from the Colima Volcanic Complex, Mexico, which is comparable to the water abundance (1 wt%) of olivine-hosted melt inclusion with a similar major element composition (Sample CU-01-05: $SiO_2 = 55.7$ wt%; Vigouroux et al. 2008) from the same volcanic complex. This suggests that the six andesites from Luhr and Carmichael (1980) likely have ~1 wt% H₂O prior to eruption. FTIR and ion probe analyses reveal < 0.5 wt% H₂O in olivine-hosted melt inclusions from the Kilauea Volcano, Hawaii (Anderson and Brown 1993; Barsanti et al. 2009), supporting nominally anhydrous pre-eruptive basaltic lavas from this volcano (Norman et al. 2005), perhaps with ~ 0.5 wt% H₂O. Ion probe analyses of plagioclase-hosted melt inclusions indicate $\sim 0.6 \pm 0.2$ wt% H₂O in the pre-eruptive dacite lavas from White Island, New Zealand (Wardell et al. 2001; Severs et al. 2009). By contrast, FTIR analyses of melt inclusions (Marianelli et al. 2006) suggest 4 ± 1 wt% H₂O in the pre-eruptive trachyphonolitic lava from Campi Flegrei, Italy (Fedele et al. 2009, 2015).

However, water contents have not been determined for phenocryst-hosted melt inclusions from Twin Peaks at Utah, the Farallón Negro Volcanic Complex at Argentina, and the Villarrica Volcano at Chile. The small to trace amount of biotite and the low H₂O contents (0.09–0.56 wt%) in the rhyolites from Utah (Nash and

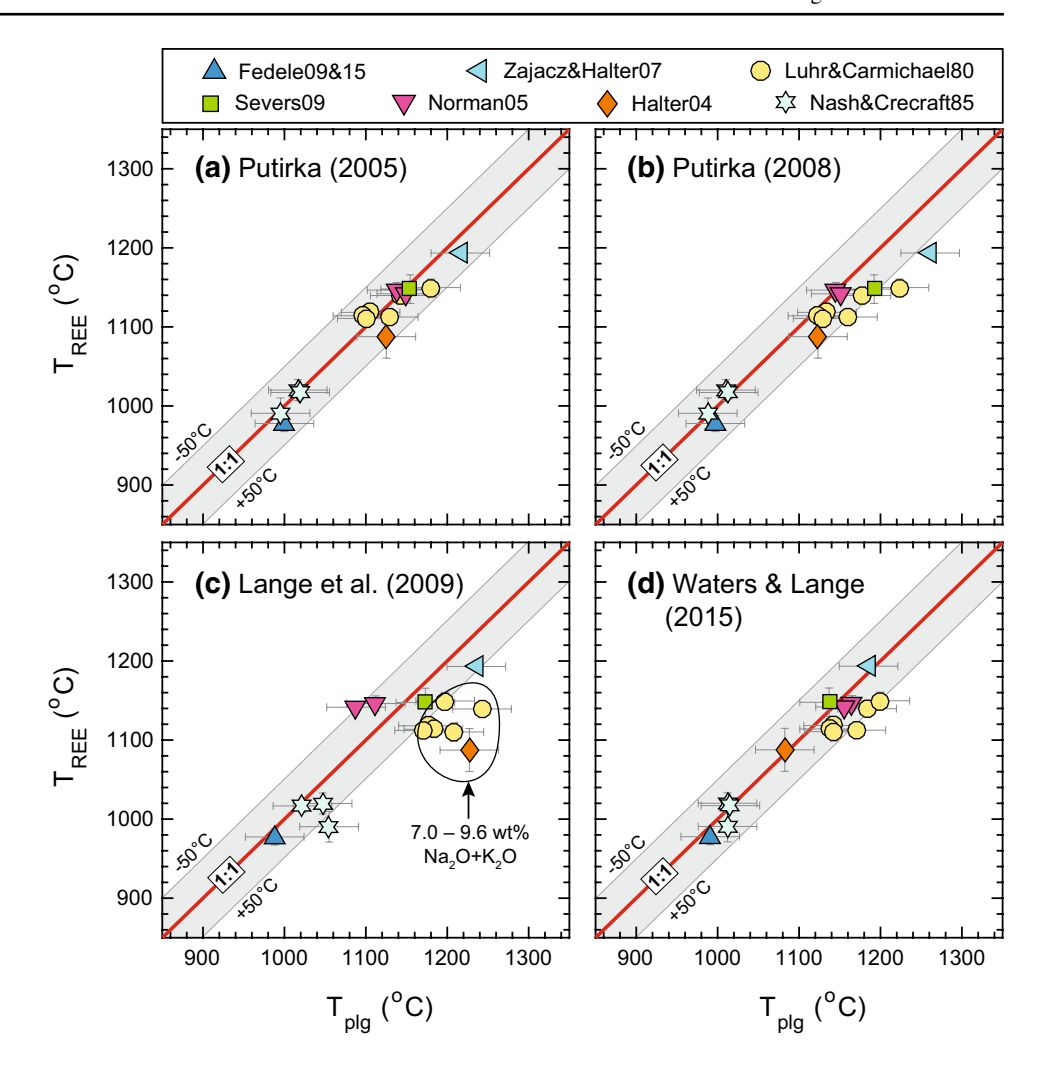


Using these estimated water contents in pre-eruptive lavas and the reported compositions of plagioclase and melt (quenched glasses or melt inclusions), we applied four plagioclase-melt thermometers (Putirka 2005, 2008; Lange et al. 2009; Waters and Lange 2015) and calculated the plagioclase crystallization temperatures at 2 kbar. According to the measured volatile contents in olivine-hosted melt inclusions (Barsanti et al. 2009), an average pressure of 0.2 kbar was used for the two basalts from Norman et al. (2005). Temperatures were also calculated for coexisting plagioclase and clinopyroxene using the REE-in-plagioclase-clinopyroxene thermometers. Results of the temperature calculations for individual samples are shown in supplementary Fig. S3. Encouragingly, temperatures derived from the REE-based thermometer (designated as T_{REE} hereafter) agree well with the crystallization temperatures calculated using different plagioclase-melt thermometers (Fig. 7). The temperature differences are generally within ± 50 °C, comparable to the calibration errors of the plagioclase saturation thermometers. Notably, the thermometer of Lang et al. (2009) produces > 50 °C higher temperatures for the andesites reported in Halter et al. (2004) and in Luhr and Carmichael (1980). Given the abundant alkaline contents in these andesites ($Na_2O + K_2O = 7.0 - 9.6$ wt%), the higher temperatures derived from Lange et al.'s thermometer are likely due to the model limitations for alkaline-rich magmas (see Fig. 5 in Waters and Lange 2015). The overall agreement between the REE-based thermometer and the plagioclase saturation thermometers indicates that temperatures calculated using the REE-in-plagioclase-clinopyroxene thermometer are the crystallization temperatures of plagioclase in pre-eruptive magmas.

The abundances of MgO in plagioclase were also reported in five samples from four studies (Halter et al. 2004; Norman et al. 2005; Zajacz and Halter 2007; Severs et al. 2009), which allow us to calculate temperatures using the Mg-exchange thermometer of Faak et al. (2013). Using the Mg-based thermometer and the parameterized temperature-dependent silica activity model from Faak et al. (2014), we calculated temperatures for individual volcanic samples. For the two Hawaii basalts (Norman



Fig. 7 Comparisons of temperatures calculated using the REE-in-plagioclase-clinopyroxene thermometer (T_{REE}) and the plagioclase-melt saturation thermometers (T_{plg}) for volcanic rocks reported in the literature. Error bars represent the standard errors of the plagioclasemelt saturation thermometers and of the temperature inversion. Grey regions illustrate the $\pm 50\,^{\circ}\text{C}$ differences



et al. 2005), temperatures derived from the Mg-exchange thermometer (KIL55-2: 1140°C; KIL55-8: 1146°C) are comparable to those derived from the REE-based thermometer $(1147 \pm 10 \,^{\circ}\text{C} \text{ and } 1144 \pm 3 \,^{\circ}\text{C}, \text{ respectively})$. The two exchange thermometers also give rise to similar temperatures for the dacite sample from New Zealand (Severs et al. 2009; $T_{Mg} = 1170 \,^{\circ}\text{C}$; $T_{REE} = 1150 \pm 6 \,^{\circ}\text{C}$). However, for the two basaltic andesites from Argentina (Halter et al. 2004) and Chile (Zajacz and Halter 2007), temperatures derived from the Mg-exchange thermometer (971 °C and 1031 °C) are significantly less than those derived from the REE-based thermometer $(1088 \pm 23 \,^{\circ}\text{C} \text{ and } 1198 \pm 4 \,^{\circ}\text{C})$. Because the pre-eruptive lavas of these two samples contain~2 wt% water, the significant temperature differences may be due to uncertainties of the silica activity model of Faak et al. (2014) that does not include the water effect. Combining with a recent activity model for hydrous silicate melts (Carmichael 2004), the Mg-exchange thermometer provides temperatures 1016°C and 1087°C for the Argentina and Chile basaltic andesites, respectively. These temperatures are still considerably smaller than the REE-recorded temperatures. One possible explanation for the discrepancy here is diffusive resetting of Mg in plagioclase, perhaps, in shallow magma chambers.

Cumulate rocks

From the literature, we compiled 70 mafic cumulate rocks with major and trace element compositions of coexisting plagioclase and clinopyroxene. These include 34 cumulates from the Sept Iles layered intrusion, Canada (Namur et al. 2011) and 36 cumulates from the Bushveld Complex, South Africa (VanTongeren and Mathez 2013; Tanner et al. 2014). The Sept Iles cumulates include 9 troctolites, 9 anorthosites, and 10 gabbros from the lower Layered Series (MCU I) and 6 anorthosites from the Upper Border Series (UBS). Major element zonations were reported for plagioclases from the anorthosite samples, which display mild core-to-rim variations (An₆₀₋₆₈). Plagioclase and clinopyroxene in the Sept Iles cumulates display a relatively small range of composition (An =48-68 in plagioclase; Mg# = 66-78 and $X_{\rm Al}^{\rm T}=0.06-0.11$ in clinopyroxene). Fine-grained



rocks from the chilled margin suggest that the parental magma of the Sept Iles Layered Series was a ferrobasalt $(SiO_2 = 48.56 \text{ wt\%}, TiO_2 = 2.85 \text{ wt\%}, \text{ and MgO} = 5.47 \text{ wt\%})$ compositionally comparable to the Skaergaard parental magma (see Table 10 in Namur et al. 2010). Hence, crystallization temperatures of the 28 cumulate rocks from Sept Iles Layered Series can be estimated using the An-based thermometer of Thy et al. (2009) that was calibrated specifically for the Skaergaard intrusion.

The 36 Bushveld cumulates include 1 anorthosite, 18 gabbronorites or gabbros from the Upper and Upper Main Zones (UUMZ) in the Eastern Limb (VanTongeren and Mathez 2013) and 1 troctolite, 2 anorthosites, and 14 gabbronorites or gabbros from the UUMZ in the Northern Limb (Tanner et al. 2014). Plagioclase and clinopyroxene in the 36 Bushveld cumulates are compositionally similar to those from the Sept Iles intrusion but display slightly larger ranges (An = 45-76 in plagioclase; Mg# = 47-84and $X_{A1}^{T} = 0.03-0.07$ in clinopyroxene). Given the continuously evolving compositions, VanTongeren and Mathez (2013) suggested that UUMZ above the Pyroxenite Marker in the Eastern Limb crystallized from a single magma composition represented by fine-grained gabbros from the chilled margin ($SiO_2 = 49.72$ wt%, $TiO_2 = 0.81$ wt%, and MgO=6.08 wt%; Davies and Cawthorn 1984). Although no such a Pyroxenite Marker is observed in the Northern Limb, the stratigraphy units and chemical fractionation trends of the Northern Limb are comparable with those of other lobs (Ashwal et al. 2005), indicating that the UUMZ parental magmas of the Northern Limb are likely similar to

that in the Eastern Limb. Assuming that plagioclase An₇₅ crystallized at 1150°C, VanTongeren and Mathez (2013) obtained a linear expression relating An in plagioclase (=55–75) to plagioclase crystallization temperature using a slope of 6.8 °C/An from MELTS (Ghiorso and Sack 1995). Because the liquidus temperature determined by MELTS is about 1200 °C at the FMQ buffer for the saturation of plagioclase An₇₅ in the suggested parental magma, we modified this An-based plagioclase thermometer accordingly to estimate crystallization temperatures of these Bushveld cumulate rocks.

Using the reported compositions of coexisting plagioclase and clinopyroxene, we applied the REE- and the Mgexchange thermometers to all compiled cumulate rocks. Three choices of pressures 1 atm, 1 kbar, and 2 kbar were used in the REE-based thermometer. Because a decrease of the assumed pressure from 2 kbar to 1 atm marginally reduces the calculated temperatures (by 2–3 °C, Fig. 6b), only the results for 2 kbar are discussed here (see individual temperature inversions in supplementary Fig. S4). The parameterized silica activity model from Faak et al. (2014) was used in the Mg-exchange thermometer for these cumulate rocks.

For mafic cumulates from the Sept Iles lower Layered Series (MCU I), temperatures derived from the REE-based thermometer generally agree with plagioclase crystallization temperatures calculated using the An-based thermometer (Thy et al. 2009) (Fig. 8a). The Sept Iles anorthosites from UBS show systematically lower REE temperatures. Because UBS anorthosites are interpreted as the result of

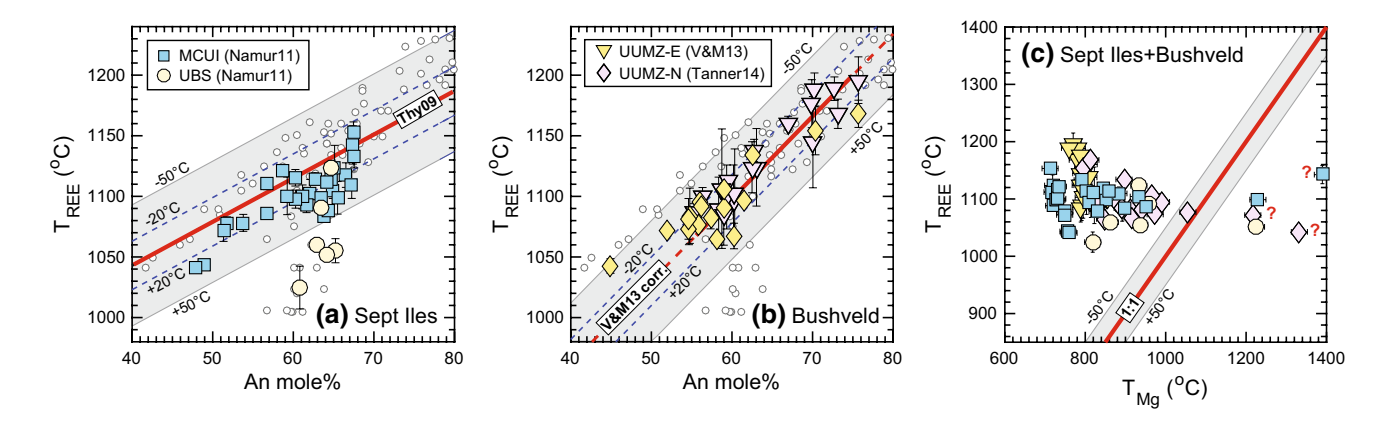


Fig. 8 Comparisons of temperatures calculated using the REE-inplagioclase-clinopyroxene thermometer (T_{REE}), the empirical Anbased plagioclase thermometers (Thy et al. 2009; VanTongeren and Mathez 2013), and the Mg-exchange thermometer of Faak et al. (2013; T_{M_0}) for cumulate rocks from the Sept Iles intrusion and the Bushveld Complex. Open circles in (a) and (b) denote the low-pressure experimental data, as shown in Fig. 1a. Question markers indicate that samples with abnormally high temperatures derived from

the Mg-exchange thermometer. Mineral compositions of the Sept Iles samples are from Namur et al. (2011), while those of the Bushveld samples are from VanTongeren and Mathez (2013) and Tanner et al. (2014). Note that we modified the An-based thermometer of VanTongeren and Mathez (2013) using the liquidus temperature (1200°C; An =75) determined by MELTS for the proposed parental magma composition in VanTongeren and Mathez (2013)



plagioclase floatation (Namur et al. 2011), their lower REEderived temperatures may be attributed to significant interaction with shallow magmas during plagioclase floatation or, perhaps, to late crystallization of interstitial clinopyroxene. However, the latter require crystallization of clinopyroxene to be delayed by more than 40% solidification after plagioclase saturation (cf. Fig. 6c).

For the Bushveld cumulates, temperatures derived from the REE-based thermometer agree well with the modified An-based thermometer of VanTongeren and Mathez (2013) (Fig. 8b), and the relative differences are generally within ± 20 °C. One sample with plagioclase An₄₅ appears to have a REE temperature about ~50 °C above the line defined by the An-based thermometer. As this An-based thermometer is calibrated for An_{55-75} , the large temperature difference for this sample is likely due to significant extrapolation of the An-based thermometer. In the REE temperature inversion diagrams (supplementary Fig. S3), many of the Bushveld samples reported by VanTongeren and Mathez (2013) display REE patterns rotated from lines passing through the origin. These rotations may be attributed partially to crystallization of plagioclase and clinopyroxene at different times or differential diffusive resetting of REE for slowly cooled samples. However, neither appears to generate rotations (cf. supplementary Figs. S2 and S5) as large as those observed for these Bushveld samples. Given that no heavy REE were reported for plagioclase from these samples, it is difficult to fully assess the origin of rotations in the temperature inversion diagrams, which require more future work.

The overall good agreement between temperatures derived from the REE-based thermometer and magma crystallization temperatures independently constrained by the An-based thermometers demonstrates that the REE-inplagioclase-clinopyroxene thermometer provides magma crystallization temperatures for the Sept Iles and Bushveld cumulate rocks. However, temperatures derived from the Mg-exchange thermometer are systematically lower than those from the REE-exchange thermometer, except six samples with abnormally high temperatures (1217–1431 °C) derived from the Mg-based thermometer (Fig. 8c). Because these values are greater than the crystallization temperatures (996-1142 °C) of the six samples constrained by Anbased thermometers, the abnormal Mg temperatures seem to be erroneous, perhaps, due to analytical issues. As Mg is readily reset in coexisting plagioclase and clinopyroxene due to fast diffusion in plagioclase (Faak et al. 2014), the overall temperature differences are consistent with the slower diffusion of REE in plagioclase and clinopyroxene. Further assessment of the kinetic effect on the REE- and Mg-based thermometers requires quantitative understanding of the extent of REE and Mg diffusive re-distribution in the coexisting plagioclase and clinopyroxene.

Discussion

Physical meaning of the calculated temperatures

The rate of diffusive exchange of an element in a cooling petrological system decreases with decreasing temperature and effectively vanishes after a certain time. The corresponding temperature is called closure temperature (T_c ; Dodson 1973), which can be determined by thermometers based on the equilibrium exchange of the element of interest (e.g., REE and Mg). In cooling cumulate rocks, diffusive exchange takes place subsequent to crystallization, so the initial temperature is approximately the mineral crystallization temperature. When the closure temperature and the initial temperature are determined independently, their difference can be used to assess the thermal history of the rock (e.g., cooling rate and residence time). A similar concept has also been used in Chin et al. (2012) to infer the P-T trajectories of cooling peridotite xenoliths.

For diffusive exchange between a crystal and a homogeneous infinite reservoir, Dodson (1973) gave a simple expression for the closure temperature of an element of interest in the crystal:

$$T_c = \frac{E/R}{\ln\left[\frac{RT_c^2 \mathbb{D}_0}{E(dT/dt)r^2}\right] + \Gamma},\tag{7}$$

where E and \mathbb{D}_0 are the activation energy and pre-exponential factor for diffusion of the element of interest; r is the effective grain radius; dT/dt is the absolute value of cooling rate at the closure temperature; and Γ is the closure function depending upon crystal geometry and location in the crystal. The spatially weighted average of Γ is 4.0066 for sphere, 3.29506 for cylinder, and 2.15821 for plane sheet. To extend Dodson's equation for arbitrary small amount of diffusion, Ganguly and Tirone (1999) modified the closure function by adding a numerical correction that is a function of the initial temperature and crystal geometry. This correction is essential for slow diffusing species (e.g., REE) and is also important for fast diffusing species (e.g., Mg) during rapid cooling. The closure problem formulated by Dodson (1973) is based on the assumption that the surrounding medium (mineral or/and melt) serves as an infinite reservoir for the crystal in question, which has to be justified for specific petrological systems.

In general, the extent of diffusive re-distribution between two coexisting minerals for an element of interest in a cooling closed bi-mineralic system depends on the diffusion parameters (activation energy and pre-exponential factor), thermal history (cooling rate and initial temperature), crystal properties (crystal size, geometry, and proportion), and partition coefficients (e.g., Dodson 1973; Lasaga et al. 1977; Eiler et al. 1992; Ehlers and Powell 1994; Ganguly



and Tirone 1999; Watson and Cherniak 2013; Liang 2014, 2015; Yao and Liang 2015). Liang (2015) provided an analytical expression for the closure temperature of a trace element in cooling bi-mineralic systems that have not been open to mass transfer with their surrounding media since their formation. Although it does not incorporate the cases with arbitrary small amount of diffusion, this generalized equation allows one to assess the relative importance of individual minerals for determining the closure temperature of a trace element in the cooling bi-mineralic system.

To facilitate discussion, here, we introduce two shorthand notations (Θ and ω) and rewrite Eq. (10) in Liang (2015) for the closure temperature of a trace element in a cooling bi-mineralic system as follows:

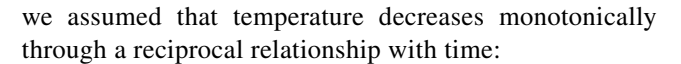
$$T_{c} = \frac{E_{\alpha}/R}{\ln\left[\frac{RT_{c}^{2}\mathbb{D}_{0}^{\alpha}}{E_{\alpha}(dT/dt)r_{\alpha}^{2}}\right] + \Gamma + \ln\left(\Theta\right)},$$
(8a)

$$\Theta = \frac{1 + \phi_r D_c}{1 + \phi_r D_c \omega},\tag{8b}$$

$$\omega = \frac{\mathbb{D}_c^{\alpha}}{\mathbb{D}_c^{\beta}} \frac{r_{\beta}^2}{r_{\alpha}^2} \left(\frac{E_{\beta} + BR}{E_{\alpha}} \right) - \frac{BR}{E_{\alpha}}, \tag{8c}$$

where Θ is a correction factor for the effects of diffusion, partitioning, and mineral proportion; ω denotes the relative diffusion rates in minerals α and β ; \mathbb{D}_{α} is the trace element diffusion coefficient for each mineral at the closure temperature; D_c is the partition coefficient at the closure temperature; ϕ_r indicates the relative mineral proportions $(\phi_{\alpha};\phi_{\beta})$ in the system. Notably, the variation of Θ strongly depends on the relative diffusion rates in individual minerals (ω): $\Theta = 1$ when $\omega = 1$; $\Theta > 1$ when $\omega < 1$; and $\Theta < 1$ when $\omega > 1$. As Θ approaches unit, Eq. (8a) is reduced to Dodson's equation (Eq. 7), and mineral β effectively serves as an infinite reservoir for trace element diffusion in mineral α . This is obviously not the case when Θ significantly deviates from unit ($|\Theta - 1| > 0$). Because the diffusion coefficients of Mg and REE in clinopyroxene are about one to three orders of magnitude less than those in plagioclase (cf. Fig. 1b), the values of ω are ~10 to ~10³ (i.e., Θ << 1) for a typical gabbro with similar proportions and grain sizes of plagioclase and clinopyroxene. Thus, the formulations of Dodson (1973) and Ganguly and Tirone (1999) are inadequate in calculating closure temperature of Mg or REE in cooling plagioclase-clinopyroxene systems, which is further examined numerically in the following discussion.

Using the Crank-Nicolson finite difference scheme, we modeled REE and Mg diffusion in two plagioclase-clinopyroxene aggregates (50:50 and 95:5) with a uniform grain radius (1 mm). Following Dodson's formulation,



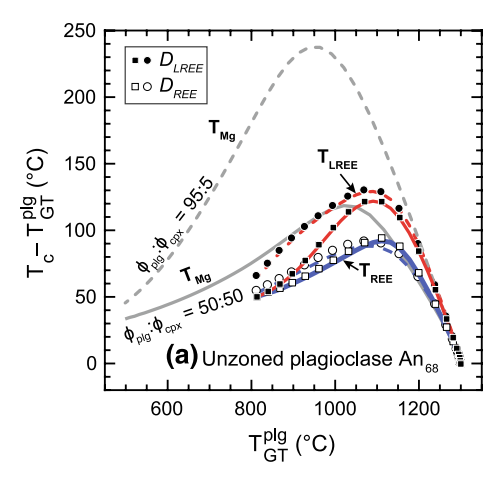
$$\frac{1}{T} = \frac{1}{T_0} + \eta \cdot t,\tag{9a}$$

$$\eta = \frac{1}{T_0^2} \frac{dT}{dt} \Big|_{T_0} = \frac{1}{T_c^2} \frac{dT}{dt} \Big|_{T_c},\tag{9b}$$

where T_0 is the initial equilibrium temperature (1300 °C) and η is a constant depending upon the cooling rate (10⁻⁸ to 10⁶ °C/yr) at the initial temperature. REE and Mg concentrations at the mineral interface were constrained by their partition coefficients and conservation of total diffusive flux. According to Yao and Liang (2015), we defined REE closure temperatures in the bi-mineralic systems through effective partition coefficients (i.e., ratios of spatially averaged concentrations in the two minerals) that are expected to be comparable with temperatures recorded by the REE-exchange thermometer. When diffusive exchange of REE between the two minerals becomes closed, we calculated temperatures by applying the REE-exchange thermometer to all REE and to only light REE, respectively. Because middle and heavy REE in plagioclase are often below the detection limits (cf. Fig. 5a), the latter are more relevant to published field data. Mg closure temperatures of the bi-mineralic system were then calculated using the Mg-exchange thermometer when diffusive exchange of Mg between the two minerals effectively vanishes. The diffusion data of REE and Mg are the same as those shown in Fig. 1b. Major element compositions of plagioclase and clinopyroxene were taken from Namur et al. (2011; DC-9-2410: An =68) for diffusion simulation. As the dominant compositional factor for the partitioning of REE (cf. Eq. 6b) and Mg (see Faak et al. 2013), Ca in plagioclase is extremely resistant to diffusive modification after plagioclase crystallization due to the slow diffusion of CaAl-NaSi in plagioclase (e.g., Grove et al. 1984). Accordingly, diffusive exchange of major element compositions is considered to be unimportant for REE and Mg diffusion. For comparison, we also calculated REE and Mg closure temperature in a single plagioclase crystal using the equation of Ganguly and Tirone (1999).

As expected, temperatures calculated using the REE-exchange thermometer (T_{REE} : blue curves in Fig. 9a) are consistent with the closure temperatures defined by the effective partition coefficients (D_{REE} : white markers) that were recommended by Yao and Liang (2015) to represent closure temperatures of cooling bi-mineralic systems. An example of temperature inversion using the REE-exchange thermometer is shown in supplementary Fig. S5 for a cooling rate of 10^{-5} °C/yr. When only light REE are available, temperatures calculated using the REE-exchange





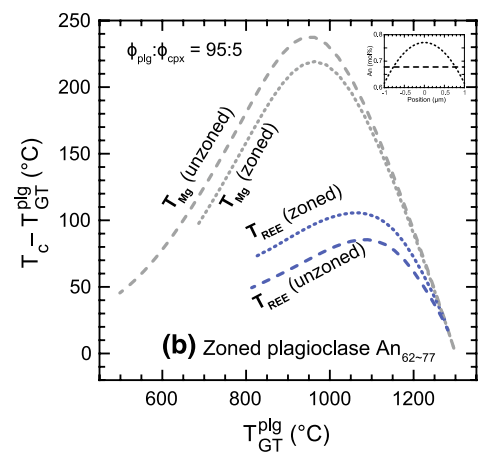


Fig. 9 Comparisons of plagioclase-clinopyroxene closure temperatures (T_c) derived from diffusion modeling and plagioclase closure temperatures calculated using the formulation of Ganguly and Tirone (1999 $T_{\rm GT}^{\rm plg}$). The mineral proportions (ϕ) in the two aggregates correspond to a gabbro ($\phi_{\rm plg}$: $\phi_{\rm cpx} = 50:50$; *solid* curves) and an anorthosite ($\phi_{\rm plg}$: $\phi_{\rm cpx} = 95:5$; *dashed* curves). Plagioclase–clinopyroxene closure temperatures in (**a**) were derived from diffusion modeling for the two aggregates with constant plagioclase composition (An =68), and

those for the anorthosite analogy in (b) were compared with results of diffusion modeling for an imposed An gradient in plagioclase (An =62–77; dotted curves). Markers show mean closure temperatures of REE defined by their effective partition coefficients. Red and blue curves denote mean closure temperatures of REE ($T_{\rm REE}$: blue) and light REE ($T_{\rm LREE}$: red) recorded by the REE-exchange thermometer. Grey curves represent closure temperatures recorded by the Mg-exchange thermometer

thermometer (T_{LREE} : red curves) become the mean closure temperatures of light REE in the plagioclase–clinopyroxene aggregates defined by the effective partition coefficients (D_{LREE} : black markers). Due to the slower diffusion rate in clinopyroxene, mean closure temperatures of light REE are systematically higher than those of all REE. Notably, both REE and Mg closure temperatures are significantly greater than those derived from the equation of Ganguly and Tirone (1999), especially when clinopyroxene becomes a minor phase. Overall, the simulation results are consistent with the closure temperature analysis based on Eq. (8) and confirm the inadequacy of the one-mineral Dodson type equation (e.g., Ganguly and Tirone 1999) in quantifying diffusive responses of REE and Mg in coexisting plagioclase and clinopyroxene in a closed system.

The preceding discussion on closure temperatures in plagioclase-clinopyroxene systems is based on tracer diffusion of REE and Mg in the two minerals. As discussed in Costa et al. (2003) for Mg diffusive exchange between plagioclase crystals and silicate magmas, the presence of major element concentration (i.e., An) gradients in plagioclase induces additional diffusive fluxes for the trace elements. However, the effect of An zonation does not appear to be significant on the closure temperatures of REE and Mg in the plagioclase–clinopyroxene systems calculated using the average An (cf. Fig. 9b; See detailed discussion in the online Supplementary Materials).

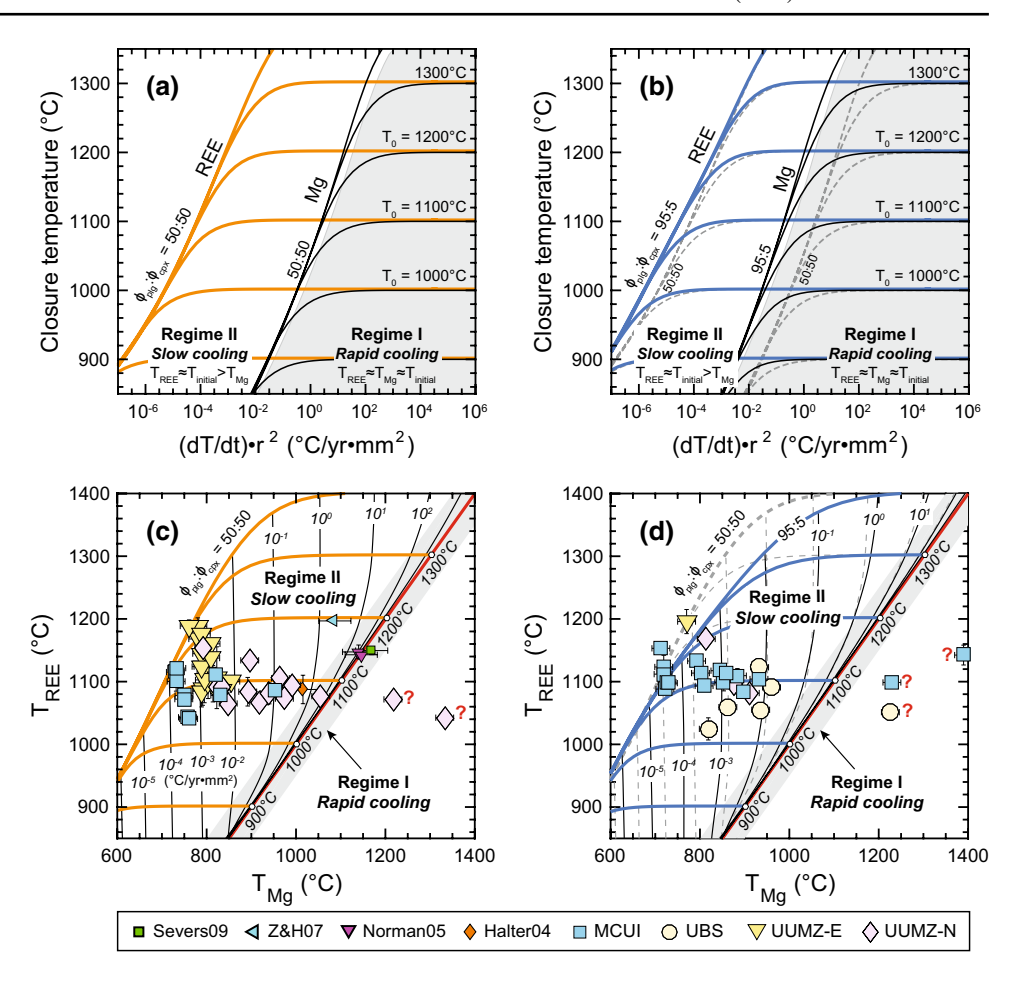
Regime diagrams for reading thermal histories

The systematic differences in temperatures derived from the REE- and Mg-exchange thermometers for the cumulate rocks can be used to deduce thermal histories of plagioclase- and clinopyroxene-bearing rocks. To illustrate the diffusive responses of REE and Mg closure temperatures to various cooling rates and initial temperatures, we numerically simulated REE and Mg diffusion in two plagioclase-clinopyroxene aggregates (50:50 and 95:5) for a range of cooling rates $(10^{-7} \text{ to } 10^7 \text{ °C/yr})$, grain radii (0.1)to 10 mm), and initial temperatures (900 to 1400 °C) using the finite difference method outlined in section "Physical meaning of the calculated temperatures". The effective diffusion radius was assumed to be uniform in the aggregates. Due to the challenge in accurate analysis of middle and heavy REE in natural plagioclase (cf. Fig. 5), the REE-inplagioclase-clinopyroxene thermometer, when applied to natural rocks, often records the closure temperature of light REE. Thus, the mean closure temperatures of light REE derived from the numerical simulations are taken as the measurable REE closure temperatures.

Figure 10a, b shows the calculated closure temperatures of REE and Mg for selected initial temperatures (900, 1000, 1100, 1200, and 1300 °C) as a function of the product of cooling rate and square grain radius. Because of the reciprocal relationship between the cooling rate and grain size $(dT/dt \propto 1/r^2$; Eqs. 7 and 8a), the product of these two serves as a single variable. The two representative mineral proportions yield comparable REE closure temperatures



Fig. 10 Plots showing REE and Mg closure temperatures in plagioclase-clinopyroxene systems as a function of cooling rate (a, b) and the regime diagrams for determination of cooling rates and initial temperatures (c, d). The closure temperatures were obtained by applying the REEand Mg-exchange thermometers to modeling results of light REE diffusive exchange between plagioclase and clinopyroxene for two choices of mineral proportions relevant to gabbros (ϕ_{plg} : $\phi_{\text{cpx}} = 50:50$; **a, c**) and anorthosites (ϕ_{plg} : ϕ_{cpx} = 95:5; **b**, **d**). Numbers along the thinner curves in (c, d) denote the products of cooling rate and square grain radius (°C/ $yr \cdot mm^2$). For comparison, the calculated closure temperatures in (a) and (c) are shown as dashed curves in (b) and (d). respectively. Markers in (c) show the compiled volcanic and gabbroic rocks, while those in (d) display the compiled troctolites and anorthosites. See Figs. 7 and 8 for marker's legends



but distinct Mg closure temperatures because of the large difference in Mg diffusion coefficients between clinopyroxene and plagioclase (Fig. 1b). The aggregate with a reduced clinopyroxene proportion displays systematically higher Mg closure temperatures.

The relative differences between REE and Mg closure temperatures lead to two characteristic regimes for rapid and slow cooling, respectively (Fig. 10c-d). The boundary between the two regimes is controlled by Mg closure temperature and vary with initial temperatures and mineral proportions. For a typical gabbro ($\phi_{\rm plg}$: $\phi_{\rm cpx}=50:50$) with an initial temperature of $1000\,^{\circ}$ C, the boundary of the two regimes is at a normalized cooling rate of $\sim 1\,^{\circ}$ C/yr \cdot mm² and moves to a faster cooling rate of $100\,^{\circ}$ C. However, for a typical anorthosite ($\phi_{\rm plg}$: $\phi_{\rm cpx}=95:5$), the boundary cooling rates become one order of magnitude smaller (e.g., $\sim 0.1\,^{\circ}$ C/yr \cdot mm² for an initial temperature of $1000\,^{\circ}$ C).

In the rapid cooling regime, REE and Mg closure temperatures are identical to the initial temperatures due to a small amount of diffusion. Because REE diffusion coefficients in plagioclase and clinopyroxene are about two to six orders of magnitude smaller than Mg diffusion coefficients in plagioclase (Fig. 1b), REE diffusive exchange is

relatively small until the cooling rate becomes very slow, whereas Mg in plagioclase can be extensively reset by diffusion for relatively slow and moderate cooling rates. Thus, in the slow cooling regime, the closure temperatures of Mg become systematically decoupled from those of REE, i.e., Mg closure temperatures decrease with the cooling rates, while REE closure temperatures remain at the initial values. When the cooling rate is slow enough to significantly reset REE and Mg in coexisting plagioclase and clinopyroxene, their closure temperatures reach the maximum difference (~450 °C) along the upper limit of the rapid cooling regime. This maximum closure temperature difference is primarily controlled by the diffusion parameters of REE and Mg and to a lesser extent the relative phase proportions, partition coefficients, and relative grain radii (Eqs. 7 and 8a-c; see also Fig. 10b). In this case, REE closure temperature represents a lower limit of possible initial temperatures. For a given cooling rate, the regime diagram (Fig. 10a-b) allows one to assess diffusive re-distribution of REE and Mg in coexisting plagioclase and clinopyroxene.

The regime diagram (Fig. 10a-b) can be converted to a plot showing the calculated REE closure temperatures against Mg closure temperatures for the selected initial



temperatures (thick curves) and a range of grain size-normalized cooling rates (thin curves; Fig. 10c-d). In this closure temperature diagram, the rapid cooling regime falls on or very close to the 1:1 correlation line, while the slow cooling regime is above the 1:1 line with an upper limit defined by the REE closure temperatures for substantial amounts of diffusion between coexisting plagioclase and clinopyroxene. This diagram is similar to that for illustrating closure temperatures of REE and major elements in two-pyroxene systems (Dygert and Liang 2015; Wang et al. 2015; Yao and Liang 2015). A useful feature of this diagram (Fig. 10c-d) is that the cooling rate and initial temperature can be directly read for a natural sample if it falls within the slow cooling regime. Assuming monotonic cooling after the initial crystallization, the cooling time from the initial temperature (or REE closure temperature) to Mg closure temperature can be further estimated using Eq. (9a). Because the estimated cooling rates also depend on the relative mineral proportions and grain sizes (cf. Eqs. 7 and 8a-c), accurate estimations of cooling rates for specific samples require diffusion modeling using relevant mineral proportions and grain sizes. In addition, care should be taken for samples near the upper bound of the slow cooling regime that indicates extensive diffusive resetting of REE in coexisting plagioclase and clinopyroxene.

In general, the initial equilibrium temperatures and cooling rates inferred from the regime diagrams are the average crystallization temperatures and average cooling rates of the bulk crystals. Because mineral cores are more resistant to diffusive resetting than rims, using only the crystal core compositions does not change the initial temperature estimates but can gives rise to an overestimation of the cooling rates by up to about one order of magnitude (see supplementary Fig. S7); however, using only the mineral rim compositions can lead to significant underestimations of the initial temperatures and cooling rates. A practical way to obtain a good approximation of the mineral average composition is to analyze multiple spots on crystals. Particularly, both crystal cores and rims should be analyzed for a better representative of the mineral average. Overgrowth rims crystalized from late stage interstitial liquids (e.g., Humphreys 2009) should be avoided.

Thermal histories of volcanic and cumulate rocks

Assuming comparable volume proportions and grain sizes of plagioclase and clinopyroxene phenocrysts, the compiled volcanic rocks are displayed in the regime diagram for ϕ_{plg} : $\phi_{\text{cpx}} = 50:50$ (Fig. 10c). The two Hawaii basalts from Norman et al. (2005) and the New Zealand dacite from Severs et al. (2009) are in the rapid cooling regime with consistent REE and Mg closure temperatures, indicating that these volcanic rocks underwent cooling at rates

of greater than $100\,^{\circ}\text{C/yr} \cdot \text{mm}^2$, i.e., $> 400\,^{\circ}\text{C/yr}$ for a 0.5 mm grain radius. The Argentina basaltic andesite from Halter et al. (2004) and the Chile basaltic andesite from Zajacz and Halter (2007) are well within the slow cooling regime. After corrections for relevant grain radii (\sim 0.5 mm and \sim 0.2 mm), the Mg closure temperatures ($1016\,^{\circ}\text{C}$ and $1087\,^{\circ}\text{C}$) suggest cooling rates of \sim 3 °C/yr and \sim 50 °C/yr for the Argentina and Chile basaltic andesites, respectively. As the Mg closure temperatures remain above solidus, the estimated cooling rates are likely related to the cooling in shallow magma chambers. Given the REE-recorded initial crystallization temperatures ($1099\,^{\circ}\text{C}$ and $1208\,^{\circ}\text{C}$), the residence times of these phenocrysts in shallow magma chambers are about 2 to 25 years.

The compiled cumulate rocks include 42 pyroxene-rich samples (gabbros and gabbronorites; $\phi_r \approx 1$) and 28 plagioclase-rich samples (troctolites and anorthosites; $\phi_r >> 1$). Assuming similar grain radii between clinopyroxene and plagioclase, these two groups are shown in the regime diagrams for $\phi_{\rm plg}$: $\phi_{\rm cpx} = 50.50$ (Fig. 10c) and $\phi_{\rm plg}$: $\phi_{\rm cpx} = 95.5$ (Fig. 10d), respectively. Excluding the six samples with abnormally high Mg-recorded temperatures (>1200 °C), most of our compiled cumulate rocks fall within the slow cooling regime in the converted regime diagrams. Near the upper bound of the slow cooling regime are five gabbroic samples (Fig. 10c) and six plagioclase-rich samples (Fig. 10d), which likely underwent diffusive resetting of both REE and Mg. For these samples, the REE-exchange thermometer only provides resetting temperatures close to crystallization. Two of the plagioclase-rich samples are above the upper limit of the slow cooling regime (Fig. 10d) and hence are inadequate for cooling rate estimations. This is, perhaps, due to more complex thermal histories rather than simple monotonic cooling (cf. Eq. 9a) or due to overestimation of initial crystallization temperatures induced by late crystallization of plagioclase (cf. Fig. 6c).

The Bushveld cumulates from the Eastern Limb display a small range of Mg closure temperatures (761-854°C), indicating normalized cooling rates at around 8×10^{-4} to 0.008 °C/yr · mm² in UUMZ. By contrast, those from the Northern Limb appear to have a broader range (794-1055 °C, excluding two anomalies > 1200 °C), suggesting normalized cooling rates of $\sim 8 \times 10^{-4}$ to ~ 5 °C/ yr · mm². Corrected for an average grain radius of 0.5 mm, the cooling rates of the Northern Limb (~ 0.003 to ~ 20 °C/ yr) appear to be faster than those of the Eastern Limb $(\sim 0.003 \text{ to } \sim 0.3 \,^{\circ}\text{C/yr})$, likely due to a smaller body of magmas emplaced in the UUMZ of the North Limb. The Bushveld cumulate B06-062 has the slowest cooling rate (~0.003 °C/yr) and suggests a maximum cooling time of ~100 kyr from a magmatic temperature 1189 $^{\circ}$ C (T_{REE}) to a subsolidus temperature 761 °C (T_{Mg}) for the Bushveld UUMZ in the Eastern Limb. Interestingly, the inferred



24

Page 18 of 20

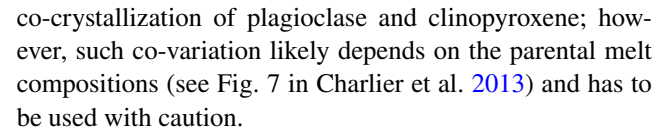
cooling time ~ 100 kyr for the Bushveld UUMZ is compatible with that for solidification of the whole Bushveld Complex derived from thermal modeling (180 kyr; Cawthorn and Webb 2013).

The Sept Iles cumulates show a wider range of Mg closure temperatures (712-960 °C, excluding four anomalies > 1200 °C), suggesting normalized cooling rates of 5×10^{-5} to $0.1 \,^{\circ}\text{C/yr} \cdot \text{mm}^2$, i.e., 2×10^{-4} to $0.4 \,^{\circ}\text{C/yr}$ for a 0.5 mm grain radius. The troctolites at the bottom of the Sept Iles intrusion appear to have the slowest cooling rate $(\sim 2 \times 10^{-4} \text{ °C/yr})$. Given their initial crystallization temperatures (1088-1123 °C) and Mg closure temperatures (718–721 °C), the estimated cooling rate indicates a maximum cooling time of ~ 1.4 Myr from magma emplacement to 721 °C. In UBS, sample M-07-22 appears to have the lowest Mg closure temperature 819 °C and hence the slowest cooling rate 6×10^{-4} °C/yr mm², i.e., 2×10^{-3} °C/yr for a 0.5 mm grain radius. Accordingly, the estimated maximum cooling time of UBS is only ~87 kyr from initial crystallization (1025 °C) to 819 °C.

Overall, the initial applications of the regime diagrams to the compiled volcanic and cumulate rocks support the conclusion that the new REE-in-plagioclase-clinopyroxene thermometer records crystallization or near-crystallization temperatures of coexisting plagioclase and clinopyroxene and also demonstrate that a combination of the REE- and Mg-exchange thermometers can place constraints on thermal and magmatic histories of crustal magma bodies.

Summary and conclusions

Crystallization temperatures of plagioclase-bearing igneous rocks are fundamental to understanding magmatic processes in crustal environments. However, magma temperatures of cumulate rocks remain difficult to constrain particularly for those derived from open magma chamber processes. We developed a new thermometer based on REE exchange between plagioclase and clinopyroxene. The temperature and composition effects were quantified through applications of the lattice strain model to plagioclase-melt and clinopyroxene-melt REE partitioning (Sun and Liang 2012; Sun et al. 2017). Several factors may influence the accuracy of this REE-exchange thermometer, including analytical errors of REE in plagioclase, uncertainties in the estimated pressure and water content, and interpretations of the crystallization sequence. Among those, the last one appears to have the most significant effect for samples from highly evolved magmas, which demands careful petrographic analyses and in situ core/rim chemical analyses. An in plagioclase and Mg# in clinopyroxene from cumulate rocks usually display a systematic co-variation (e.g., Ashwal et al. 2005) that may be used to test the



For volcanic phenocrysts from basalt, andesite, rhyolite, and phonolitic trachyte with various amounts of water, temperatures derived from the new REE-based thermometer agree well with those determined by existing plagioclasemelt thermometers. The agreement between the two different types of thermometers lends confidence to the application of the REE-in-plagioclase-clinopyroxene thermometer to felsic and hydrous systems. For mafic cumulate rocks crystalized from a single magma composition, temperatures derived from the REE-exchange thermometer are consistent with the empirical An-based thermometer that was calibrated for specific parental magma compositions. The overall agreements between temperatures recorded by the REE-exchange thermometer and independently constrained crystallization temperatures for volcanic rocks and cumulate rocks demonstrate that the REE-in-plagioclase-clinopyroxene thermometer provides crystallization or nearcrystallization temperatures of co-saturated plagioclase and clinopyroxene in shallow-level magma bodies.

Comparing with the plagioclase-clinopyroxene Mgexchange thermometer of Faak et al. (2013), the new REEexchange thermometer provides similar temperatures for volcanic rocks but yields systematically larger temperatures for cumulate rocks. The systematic differences in temperature derived from the two thermometers are related to the closure temperatures of Mg and REE in the coexisting plagioclase and clinopyroxene and are characterized by two cooling regimes. During rapid cooling (e.g., volcanic rocks), both Mg and REE thermometers tend to record the initial temperatures of mineral crystallization. During relatively slow cooling (e.g., cumulate rocks), REE in coexisting plagioclase and clinopyroxene still preserve the record of initial magmatic or near magmatic temperatures, but Mg in the bi-mineralic aggregate is reset by subsolidus diffusive re-equilibration. The distinct diffusive responses of REE and Mg to temperature changes enable quantitative constraints on thermal histories of plagioclase- and clinopyroxene-bearing igneous rocks through application of the REE- and Mg-exchange thermometers and diffusion modeling. Although the present study focuses on igneous rocks, the REE-in-plagioclase-clinopyroxene thermometer should also be applicable for estimating the early thermal histories of metamorphic rocks and planetary materials, a subject of future work.

Acknowledgements We thank Jill VanTongeren, Lewis Ashwal, Fred Roelofse, Christian Tegner, and Lijing Yao for useful discussion. Thoughtful reviews by Cin-Ty Lee and an anonymous reviewer helped to improve this manuscript. C. Sun acknowledges support from the Devonshire postdoctoral scholarship at WHOI. This work



was supported in part by the NSF grants EAR-1220076 and EAR-1632815, and NASA grant NNX13AH07G.

References

- Almeev RR, Holtz F, Koepke J, Parat F (2012) Experimental calibration of the effect of H2O on plagioclase crystallization in basaltic melt at 200 MPa. Am Mineral 97:1234–1240
- Anders E, Grevesse N (1989) Abundances of the elements: Meteoritic and solar. Geochim Cosmochim Acta 53:197–214
- Anderson AT, Brown GG (1993) CO₂ contents and formation pressures of some Kilauean melt inclusions. Am Mineral 78:794–803
- Ashwal LD, Webb SJ, Knoper MW (2005) Magmatic stratigraphy in the Bushveld Northern Lobe: continuous geophysical and mineralogical data from the 2950 m Bellevue drillcore. S Afr J Geol 108:199–232
- Barsanti M, Papale P, Barbato D, Moretti R, Boschi E, Hauri E, Longo A (2009) Heterogeneous large total CO₂ abundance in the shallow magmatic system of Kilauea volcano, Hawaii. Journal of Geophysical Research: Solid Earth 114(B12)
- Blundy J, Wood B (1994) Prediction of crystal-melt partition coefficients from elastic moduli. Nature 372:452–454
- Carmichael IS (2004) The activity of silica, water, and the equilibration of intermediate and silicic magmas. Am Mineral 89:1438–1446
- Cawthorn RG, Webb SJ (2013) Cooling of the Bushveld Complex, South Africa: implications for paleomagnetic reversals. Geology 41:687–690
- Charlier B, Grove TL (2012) Experiments on liquid immiscibility along tholeitic liquid lines of descent. Contrib Mineral Petrol 164:27–44
- Charlier B, Namur O, Grove TL (2013) Compositional and kinetic controls on liquid immiscibility in ferrobasalt–rhyolite volcanic and plutonic series. Geochim Cosmochim Acta 113:79–93
- Cherniak DJ (2003) REE diffusion in feldspar. Chem Geol 193:25–41Cherniak DJ (2010) Cation diffusion in feldspars. Rev Mineral Geochem 72:691–733
- Cherniak DJ, Dimanov A (2010) Diffusion in pyroxene, mica and amphibole. Rev Mineral Geochem 72:641–690
- Chin EJ, Lee CTA, Luffi P, Tice M (2012) Deep lithospheric thickening and refertilization beneath continental arcs: case study of the P, T and compositional evolution of peridotite xenoliths from the Sierra Nevada, California. J Petrol 53:477–511
- Costa F, Chakraborty S, Dohmen R (2003) Diffusion coupling between trace and major elements and a model for calculation of magma residence times using plagioclase. Geochim Cosmochim Acta 67:2189-2200
- Davies G, Cawthorn RG (1984) Mineralogical data on a multiple intrusion in the Rustenburg Layered Suite of the Bushveld Complex. Mineral Mag 48:469–480
- Dodson MH (1973) Closure temperature in cooling geochronological and petrological systems. Contrib Mineral Petrol 40:259–274
- Dygert N, Liang Y (2015) Temperatures and cooling rates recorded in REE in coexisting pyroxenes in ophiolitic and abyssal peridotites. Earth Planet Sci Lett 420:151–161
- Ehlers K, Powell R (1994) An empirical modification of Dodson's equation for closure temperature in binary systems. Geochimica et cosmochimica Acta 58:241–248
- Eiler JM, Baumgartner LP, Valley JW (1992) Intercrystalline stable isotope diffusion: a fast grain boundary model. Contrib Mineral Petrol 112:543–557

- Faak K, Chakraborty S, Coogan LA (2013) Mg in plagioclase: Experimental calibration of a new geothermometer and diffusion coefficients. Geochim Cosmochim Acta 123:195–217
- Faak K, Coogan LA, Chakraborty S (2014) A new Mg-in-plagioclase geospeedometer for the determination of cooling rates of mafic rocks. Geochim Cosmochim Acta 140:691–707
- Fedele L, Zanetti A, Morra V, Lustrino M, Melluso L, Vannucci R (2009) Insights on the clinopyroxene/liquid trace element partitioning in natural trachyte-trachyphonolite systems: an EMP/LA-ICP-MS case study from Campi Flegrei (southern Italy). Contrib Mineral Petrol 158:337–356
- Fedele L, Lustrino M, Melluso L, Morra V, Zanetti A, Vannucci R (2015) Trace-element partitioning between plagioclase, alkali feldspar, Ti-magnetite, biotite, apatite, and evolved potassic liquids from Campi Flegrei (Southern Italy). Am Mineral 100:233–249
- Ganguly J, Tirone M (1999) Diffusion closure temperature and age of a mineral with arbitrary extent of diffusion: theoretical formulation and applications. Earth Planet Sci Lett 170:131–140
- Ghiorso MS, Sack RO (1995) Chemical mass transfer in magmatic processes IV. A revised and internally consistent thermodynamic model for the interpolation and extrapolation of liquid–solid equilibria in magmatic systems at elevated temperatures and pressures. Contrib Mineral Petrol 119:197–212
- Glazner AF (1984) Activities of olivine and plagioclase components in silicate melts and their application to geothermometry. Contrib Mineral Petrol 88:260–268
- Grove TL, Baker MB, Kinzler RJ (1984) Coupled CaAl-NaSi diffusion in plagioclase feldspar: experiments and applications to cooling rate speedometry. Geochim Cosmochim Acta 48:2113–2121
- Halter WE, Heinrich CA, Pettke T (2004) Laser-ablation ICP-MS analysis of silicate and sulfide melt inclusions in an andesitic complex II: evidence for magma mixing and magma chamber evolution. Contrib Mineral Petrol 147:397–412
- Humphreys MC (2009) Chemical Evolution of Intercumulus Liquid, as Recorded in Plagioclase Overgrowth Rims from the Skaergaard Intrusion. J Petrol 50:127–145
- Kudo AM, Weill DF (1970) An igneous plagioclase thermometer. Contrib Mineral Petrol 25:52–65
- Lange RA, Frey HM, Hector J (2009) A thermodynamic model for the plagioclase-liquid hygrometer/thermometer. Am Mineral 94:494–506
- Lasaga AC, Richardson SM, Holland HD (1977) The mathematics of cation diffusion and exchange between silicate minerals during retrograde metamorphism. In: Saxena SK, Bhattacharji S (eds) Energetics of Geological Processes. Springer-Verlag, New York, pp 353–388
- Lee CTA, Harbert A, Leeman WP (2007) Extension of lattice strain theory to mineral/mineral rare-earth element partitioning: an approach for assessing disequilibrium and developing internally consistent partition coefficients between olivine, orthopyroxene, clinopyroxene and basaltic melt. Geochim Cosmochim Acta 71:481–496
- Liang Y (2014) Time scales of diffusive re-equilibration in bi-mineralic systems with and without a fluid or melt phase. Geochim Cosmochim Acta 132:274–287
- Liang Y (2015) A simple model for closure temperature of a trace element in cooling bi-mineralic systems. Geochim Cosmochim Acta 165:35–43
- Liang Y, Sun C, Yao L (2013) A REE-in-two-pyroxene thermometer for mafic and ultramafic rocks. Geochim Cosmochim Acta 102:246–260
- Luhr JF, Carmichael IS (1980) The colima volcanic complex, Mexico. Contrib Mineral Petrol 71:343–372



- Marianelli P, Sbrana A, Proto M (2006) Magma chamber of the Campi Flegrei supervolcano at the time of eruption of the Campanian Ignimbrite. Geology 34:937–940
- Mathez EA (1973) Refinement of the Kudo-Weill plagioclase thermometer and its application to basaltic rocks. Contrib Mineral Petrol 41:61–72
- Morse SA (2010) A critical comment on Thy et al. (2009b): Liquidus temperatures of the Skaergaard magma. Am Mineral 95:1817–1827
- Müller T, Dohmen R, Becker HW, Ter Heege JH, Chakraborty S (2013) Fe–Mg interdiffusion rates in clinopyroxene: experimental data and implications for Fe–Mg exchange geothermometers. Contrib Mineral Petrol 166:1563–1576
- Namur O, Charlier B, Toplis MJ, Higgins MD, Liégeois JP, Vander Auwera J (2010) Crystallization sequence and magma chamber processes in the ferrobasaltic Sept Iles layered intrusion, Canada. J Petrol 51:1203–1236
- Namur O, Charlier B, Pirard C, Hermann J, Liégeois JP, Vander Auwera J (2011) Anorthosite formation by plagioclase flotation in ferrobasalt and implications for the lunar crust. Geochim Cosmochim Acta 75:4998–5018
- Namur O, Charlier B, Toplis MJ, Vander Auwera J (2012) Prediction of plagioclase-melt equilibria in anhydrous silicate melts at 1-atm. Contrib Mineral Petrol 163:133–150
- Nash WP, Crecraft HR (1985) Partition coefficients for trace elements in silicic magmas. Geochim Cosmochim Acta 49:2309–2322
- Norman M, Garcia MO, Pietruszka AJ (2005) Trace-element distribution coefficients for pyroxenes, plagioclase, and olivine in evolved tholeites from the 1955 eruption of Kilauea Volcano, Hawai'i, and petrogenesis of differentiated rift-zone lavas. Am Mineral 90:888–899
- Putirka KD (2005) Igneous thermometers and barometers based on plagioclase + liquid equilibria: Tests of some existing models and new calibrations. Am Mineral 90:336–346
- Putirka KD (2008) Thermometers and barometers for volcanic systems, Rev Mineral Geochem 69:61–120
- Seitz HM, Altherr R, Ludwig T (1999) Partitioning of transition elements between orthopyroxene and clinopyroxene in peridotitic and websteritic xenoliths: new empirical geothermometers. Geochim Cosmochim Acta 63:3967–3982
- Severs MJ, Beard JS, Fedele L, Hanchar JM, Mutchler SR, Bodnar RJ (2009) Partitioning behavior of trace elements between dacitic melt and plagioclase, orthopyroxene, and clinopyroxene based on laser ablation ICPMS analysis of silicate melt inclusions. Geochim Cosmochim Acta 73:2123–2141
- Stosch HG (1982) Rare earth element partitioning between minerals from anhydrous spinel peridotite xenoliths. Geochim Cosmochim Acta 46:793–811
- Sun C, Liang Y (2012) Distribution of REE between clinopyroxene and basaltic melt along a mantle adiabat: effects of major element composition, water, and temperature. Contrib Mineral Petrol 163:807–823
- Sun C, Liang Y (2013a) Distribution of REE and HFSE between low-Ca pyroxene and lunar picritic melts around multiple saturation points. Geochim Cosmochim Acta 119:340–358
- Sun C, Liang Y (2013b) The importance of crystal chemistry on REE partitioning between mantle minerals (garnet, clinopyroxene, orthopyroxene, and olivine) and basaltic melts. Chem Geol 358:23–36
- Sun C, Liang Y (2014) An assessment of subsolidus re-equilibration on REE distribution among mantle minerals olivine, orthopyroxene, clinopyroxene, and garnet in peridotites. Chem Geol 372:80–91
- Sun C, Liang Y (2015) A REE-in-garnet-clinopyroxene thermobarometer for eclogites, granulites and garnet peridotites. Chem Geol 393:79–92

- Sun C, Graff M, Liang Y (2017) Trace element partitioning between plagioclase and silicate melt: the importance of temperature and plagioclase composition, with implications for terrestrial and lunar magmatism. Geochim Cosmochim Acta (in press). doi:10.1016/j.gca.2017.03.003
- Tanner D, Mavrogenes JA, Arculus RJ, Jenner FE (2014) Trace element stratigraphy of the Bellevue Core, Northern Bushveld: multiple magma injections obscured by diffusive processes. J Petrol 55:859–882
- Thy P, Tegner C, Lesher CE (2009) Liquidus temperatures of the Skaergaard magma. Am Miner 94:1371–1376
- Van Orman JA, Grove TL, Shimizu N (2001) Rare earth element diffusion in diopside: influence of temperature, pressure, and ionic radius, and an elastic model for diffusion in silicates. Contrib Miner Petrol 141:687–703
- Van Orman JA, Cherniak DJ, Kita NT (2014) Magnesium diffusion in plagioclase: dependence on composition, and implications for thermal resetting of the 26 Al–26 Mg early solar system chronometer. Earth Planet Sci Lett 385:79–88
- VanTongeren JA, Mathez EA (2013) Incoming magma composition and style of recharge below the pyroxenite marker, eastern Bushveld complex, South Africa. J Petrol 54:1585–1605
- Vigouroux N, Wallace PJ, Kent AJ (2008) Volatiles in high-K magmas from the western Trans-Mexican volcanic belt: evidence for fluid fluxing and extreme enrichment of the mantle wedge by subduction processes. J Petrol 49:1589–1618
- Wang C, Liang Y, Xu W (2015) On the significance of temperatures derived from major element and REE based two-pyroxene thermometers for mantle xenoliths from the North China Craton. Lithos 224:101–113
- Wardell LJ, Kyle PR, Dunbar N, Christenson B (2001) White Island volcano, New Zealand: carbon dioxide and sulfur dioxide emission rates and melt inclusion studies. Chem Geol 177:187–200
- Waters LE, Lange RA (2015) An updated calibration of the plagioclase-liquid hygrometer-thermometer applicable to basalts through rhyolites. Am Miner 100:2172–2184
- Watson EB, Cherniak DJ (2013) Simple equations for diffusion in response to heating. Chem Geol 335:93–104
- Witt-Eickschen G, O'Neill HSC (2005) The effect of temperature on the equilibrium distribution of trace elements between clinopyroxene, orthopyroxene, olivine and spinel in upper mantle peridotite. Chem Geol 221:65–101
- Wood BJ, Blundy JD (2002) The effect of H 2 O on crystal-melt partitioning of trace elements. Geochim Cosmochim Acta 66:3647–3656
- Workman RK, Hart SR (2005) Major and trace element composition of the depleted MORB mantle (DMM). Earth Planet Sci Lett 231:53-72
- Yao L, Liang Y (2015) Closure temperature in cooling bi-mineralic systems: I. Definition and with application to REE-in-two-pyroxene thermometer. Geochim Cosmochim Acta 162:137–150
- Yao L, Sun C, Liang Y (2012) A parameterized model for REE distribution between low-Ca pyroxene and basaltic melts with applications to REE partitioning in low-Ca pyroxene along a mantle adiabat and during pyroxenite-derived melt and peridotite interaction. Contrib Miner Petrol 164:261–280
- Zajacz Z, Halter W (2007) LA-ICPMS analyses of silicate melt inclusions in co-precipitated minerals: quantification, data analysis and mineral/melt partitioning. Geochim Cosmochim Acta 71:1021–1040

